High-resolution inelastic x-ray scattering

Giulio Monaco
Università di Trento (I)

outline:

- Introduction and theoretical foundation
- Instrumentation
- Selected results
- Time domain interferometry
- First applications at FELs

Scattering kinematics

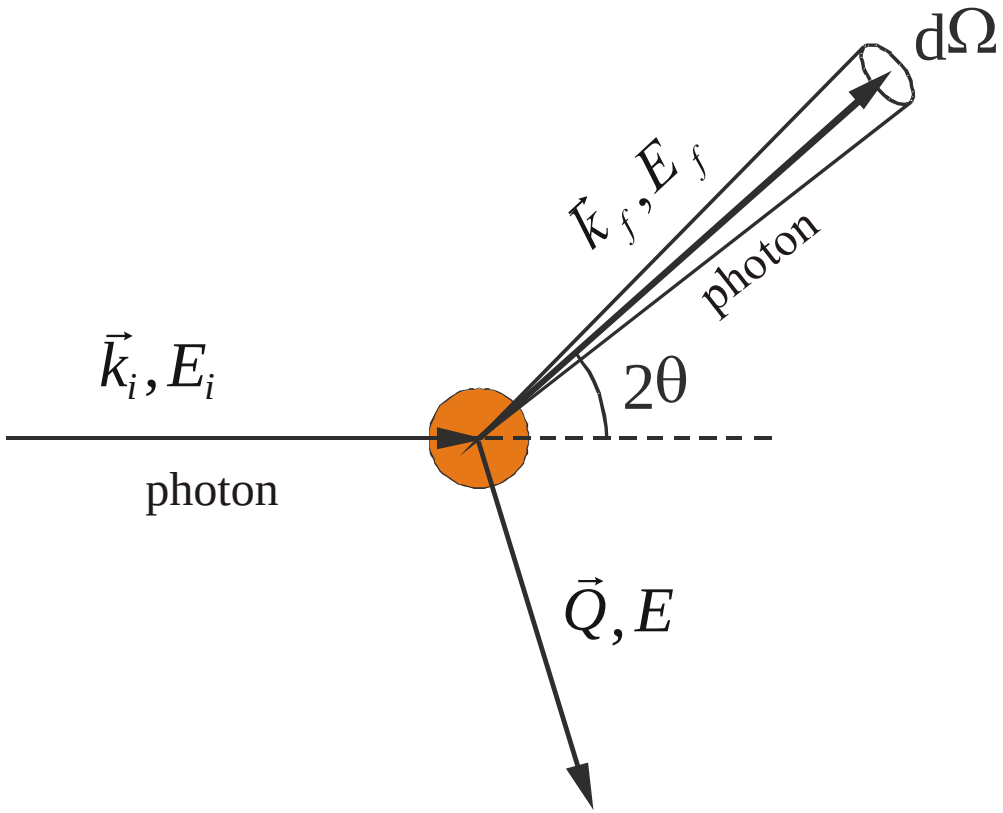

- Energy transfer: $E_i - E_f = E$
- Momentum transfer: $\vec{k}_i - \vec{k}_f = \vec{Q}$

IXS: applications - I

S(Q,ω)

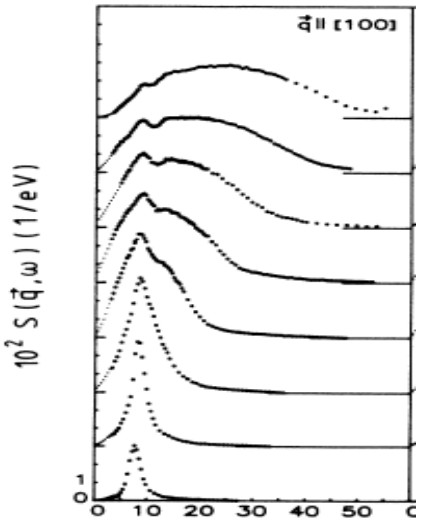

Phonons

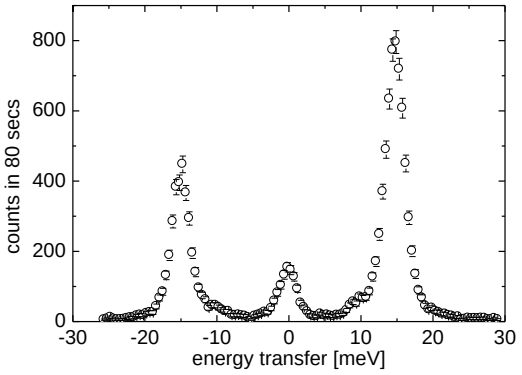

Electron dynamics $\varepsilon(\mathbf{q},\omega)$

- plasmons
- many-body phenomena
- soft X-ray absorption spectroscopy

Lattice dynamics

- elasticity
- thermodynamics
- phase stability
- e^--ph coupling

IXS: applications - II

Compton scattering

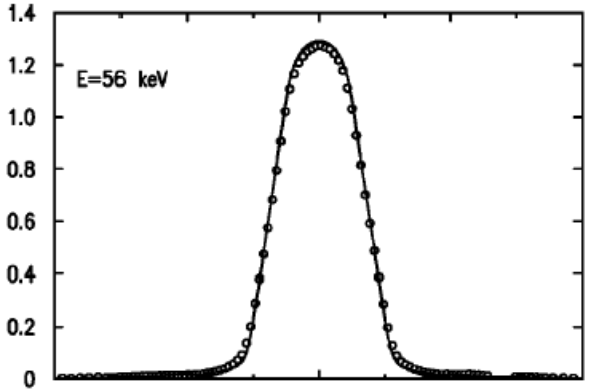

Impulse distribution of electrons

- chemical bonding
- local structures

Resonant X-ray emission

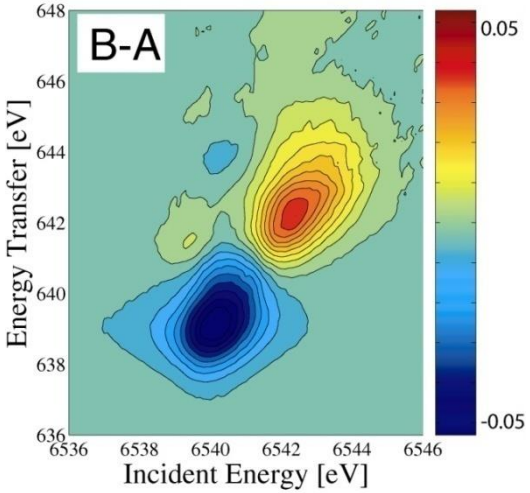

Electronic structure

- element selective
- valence selective
- spin selective

Schematic IXS spectrum

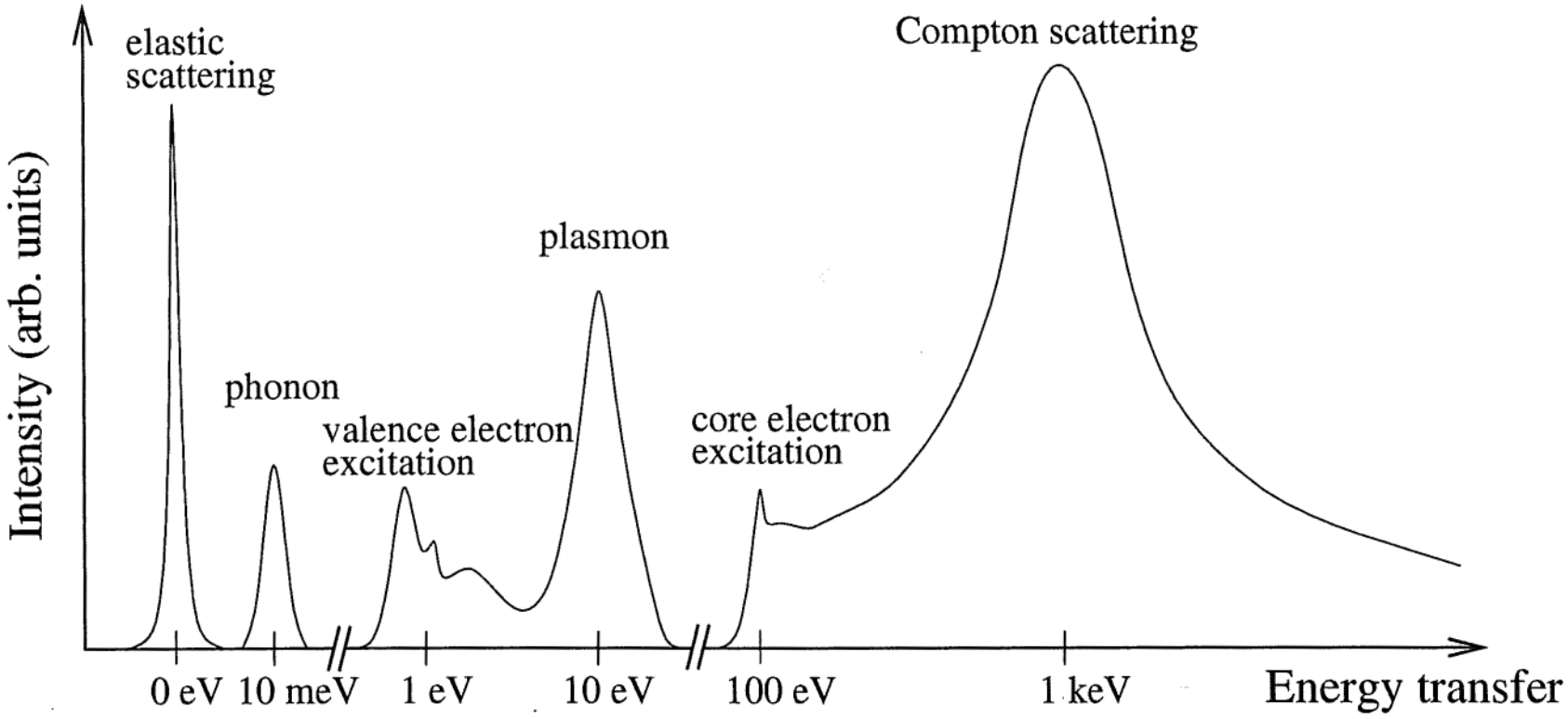

- Energy transfer: $E_i - E_f = \Delta E = 1\ \text{meV} - 1\ \text{keV}$
- Momentum transfer: $\vec{k}_i - \vec{k}_f = \vec{Q} = 1 - 180\ \text{nm}^{-1}$

Hamiltonian for the photon-electron interaction - I

The use of the following Hamiltonian within a perturbation scheme to second order in (v/c) leads to the same results of a rigorous quantum field calculation:

$$H = \sum_j \frac{1}{2m}\left[\mathbf{p}_j - \frac{e}{c}\mathbf{A}(\mathbf{r}_j)\right]^2 + \sum_{j\ j'} V(r_{j\ j'}) - \frac{e\hbar}{2mc}\sum_j \boldsymbol{\sigma}_j \cdot \nabla \times \mathbf{A}(\mathbf{r}_j) +$$

$$-\frac{e\hbar}{2mc}\sum_j \boldsymbol{\sigma}_j \cdot \mathbf{E}(\mathbf{r}_j) \times \left[\mathbf{p}_j - \frac{e}{c}\mathbf{A}(\mathbf{r}_j)\right] + \sum_{\mathbf{K}\lambda} \hbar\omega_{\mathbf{K}\lambda}\left[c^+(\mathbf{K}\lambda)c(\mathbf{K}\lambda) + \frac{1}{2}\right]$$

The vector potential operator can be expressed as:

$$\mathbf{A}(\mathbf{r}) = \sum_{\mathbf{K}\lambda} \sqrt{\frac{2\pi\hbar c^2}{V\omega_{\mathbf{K}}}}\left[e(\mathbf{K}\lambda)c(\mathbf{K}\lambda)e^{i\mathbf{K}\cdot\mathbf{r} - i\omega_{\mathbf{K}}t} + e^*(\mathbf{K}\lambda)c^+(\mathbf{K}\lambda)e^{-i\mathbf{K}\cdot\mathbf{r} + i\omega_{\mathbf{K}}t}\right]$$

with: $\mathbf{E} = -\nabla\phi - \frac{1}{c}\dot{\mathbf{A}}$ $\qquad$ $\mathbf{B} = \nabla \times \mathbf{A}$

Hamiltonian for the photon-electron interaction - II

Interaction between the radiation field and the electrons:

$$H_{i1} = \frac{e^2}{2mc^2}\sum_j \mathbf{A}^2(\mathbf{r}_j) \qquad H_{i2} = -\frac{e}{mc}\sum_j \mathbf{A}(\mathbf{r}_j)\cdot\mathbf{p}_j$$

$$H_{i3} = -\frac{e\hbar}{2mc}\sum_j \boldsymbol{\sigma}_j \cdot \left[\nabla \times \mathbf{A}(\mathbf{r}_j)\right] \qquad H_{i4} = -\frac{e^2\hbar}{4m^2c^4}\sum_j \boldsymbol{\sigma}_j \cdot \left[\dot{\mathbf{A}}(\mathbf{r}_j)\times \mathbf{A}(\mathbf{r}_j)\right]$$

Unperturbed Hamiltonian:

$$H_0 = \sum_j \frac{1}{2m}\mathbf{p}_j^2 + \sum_{j\,j'} V(r_{j\,j'}) + \frac{e\hbar}{4m^2c^2}\sum_j \boldsymbol{\sigma}_j \cdot \left(\nabla\phi \times \mathbf{p}_j\right)$$

$$H_R = \sum_{\mathbf{K}\lambda} \hbar\omega_{\mathbf{K}\lambda}\left[c^+(\mathbf{K}\lambda)c(\mathbf{K}\lambda) + \frac{1}{2}\right]$$

The Kramers-Heisenberg formula

According to Fermi's golden rule the transition probability per unit time is given to second order by:

$$w = \frac{2\pi}{\hbar}\left|\left\langle F\left|H_{i1}+H_{i4}\right|I\right\rangle + \sum_N \frac{\left\langle F\left|H_{i2}+H_{i3}\right|N\right\rangle\left\langle N\left|H_{i2}+H_{i3}\right|I\right\rangle}{(E_I-E_N)^2}\right|^2 \delta(E_I-E_F)$$

Usual definitions: $\omega = \omega_1 - \omega_2$ $\qquad$ $\mathbf{q} = \mathbf{K}_1 - \mathbf{K}_2$

Double differential scattering cross-section for the transition |i> $\rightarrow$|f>:

$$\left(\frac{\partial^2\sigma}{\partial\Omega_2\partial\hbar\omega_2}\right)_{|i\rangle\rightarrow|f\rangle} = \left(\frac{e}{mc^2}\right)^2\left(\frac{\omega_2}{\omega_1}\right)\left|\left\langle f\left|\sum_j e^{i\mathbf{q}\cdot\mathbf{r}_j}\right|i\right\rangle\left(\mathbf{e}_1\cdot\mathbf{e}_2^*\right)+A\right|^2 \delta(E_i-E_f+\hbar\omega)$$

Out of resonance, the A-term is $\hbar\omega(mc^2)^{-1}$ smaller than the Thomson one.

Thomson scattering - I

$$\frac{\partial^2\sigma}{\partial\Omega_2\partial\hbar\omega_2} = r_0^2\left(\frac{\omega_2}{\omega_1}\right)\left|\mathbf{e}_1\cdot\mathbf{e}_2^*\right|^2\sum_{i\ f}\ \sum_{j\ j'} g_i\left\langle i\left|\sum_j e^{-i\mathbf{q}\cdot\mathbf{r}_j}\right|f\right\rangle\left\langle f\left|\sum_j e^{i\mathbf{q}\cdot\mathbf{r}_{j'}}\right|i\right\rangle\ \delta(E_i - E_f + \hbar\omega)$$

with the classical electron radius: $r_0 = \frac{e^2}{mc^2} \approx 3\cdot 10^{-5}\ A$

and the dynamic structure factor:

$$S(q,\omega) = \sum_{i\ f}\ \sum_{j\ j'} g_i\left\langle i\left|\sum_j e^{-i\mathbf{q}\cdot\mathbf{r}_j}\right|f\right\rangle\left\langle f\left|\sum_j e^{i\mathbf{q}\cdot\mathbf{r}_{j'}}\right|i\right\rangle\ \delta(E_i - E_f + \hbar\omega)$$

Following van Hove, we can use another picture. We introduce the electron density operator:

$$\rho(\mathbf{r}) = \sum_j \delta(\mathbf{r} - \mathbf{r}_j) \qquad \text{or} \qquad \rho(\mathbf{q}) = \sum_j e^{-i\mathbf{q}\cdot\mathbf{r}_j}$$

Thomson scattering - II

$$S(q,\omega) = \frac{1}{2\pi\hbar}\int_{-\infty}^{+\infty} dt\; e^{-i\omega t}\left\langle \rho(\mathbf{q},0)\rho^{+}(\mathbf{q},t)\right\rangle$$

$$= \frac{1}{2\pi\hbar}\int_{-\infty}^{+\infty} dt\; e^{-i\omega t}\left\langle \sum_{i\;j} e^{-i\mathbf{q}\cdot\mathbf{r}_i(0)} e^{i\mathbf{q}\cdot\mathbf{r}_j(t)}\right\rangle$$

van Hove space-time correlation function:

$$G(\mathbf{r},t) = \sum_{j\;j'}\int d^3r'\;\left\langle \delta(\mathbf{r}'-\mathbf{r}_j(0))\;\delta(\mathbf{r}'+\mathbf{r}-\mathbf{r}_{j'}(t))\right\rangle$$

$$= \int d^3r'\;\; n_2(\mathbf{r}',\mathbf{r},t)$$

Static correlations: $$S(\mathbf{q}) = 1+\rho\int d^3r\,\left[g(\mathbf{r})-1\right] e^{-i\mathbf{q}\cdot\mathbf{r}}$$

Single crystal: selection rules

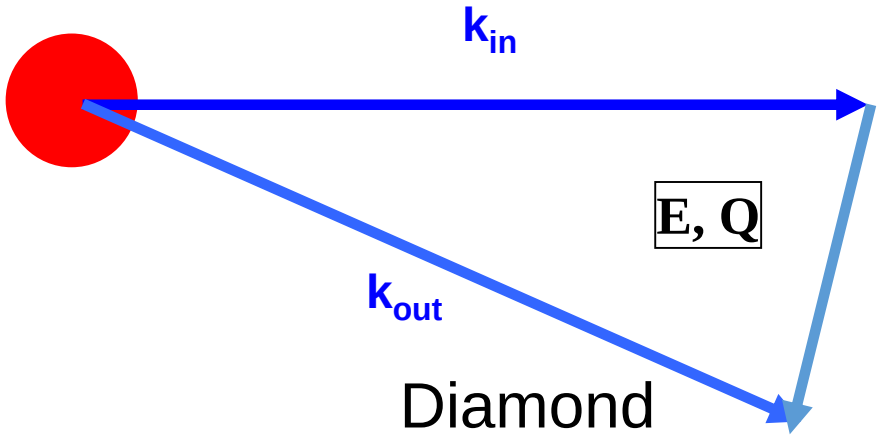

Diamond

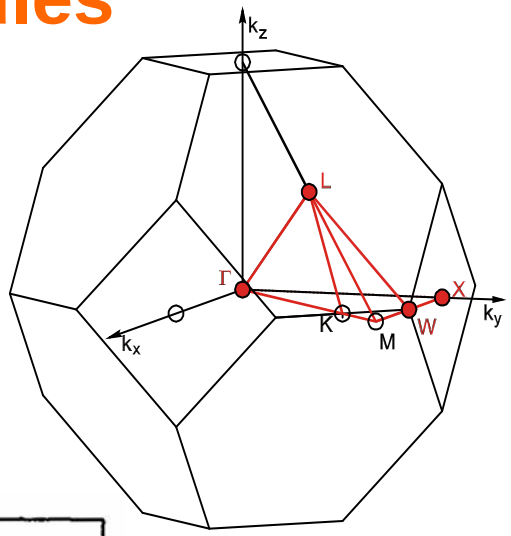

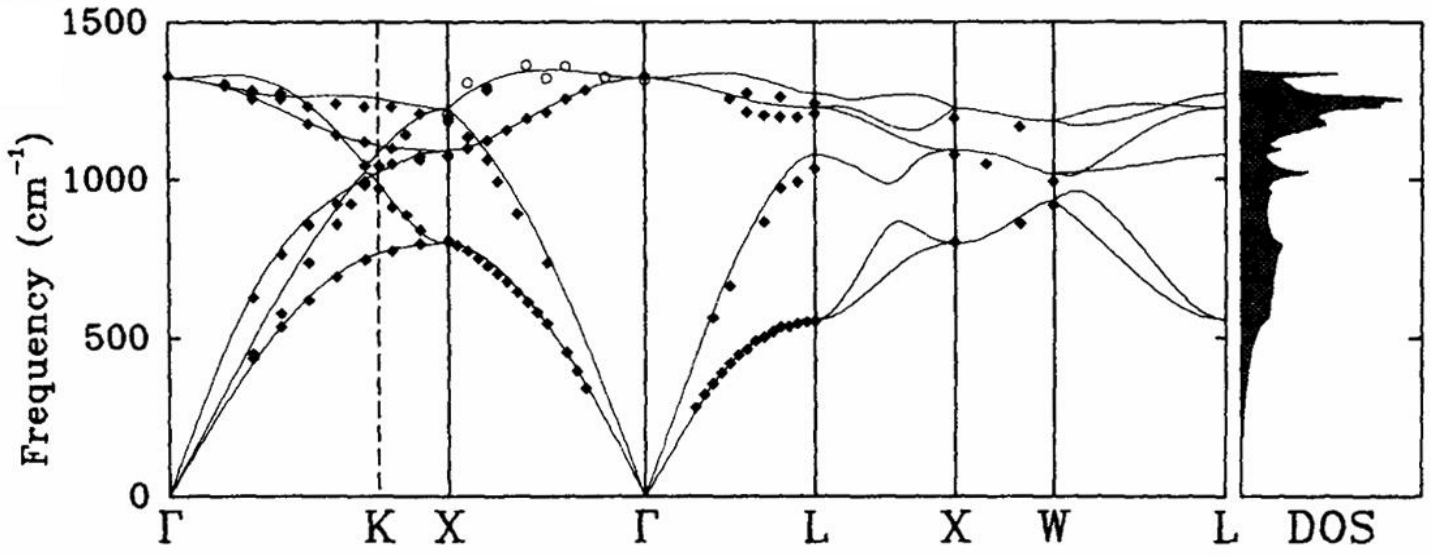

Pavone et al., PRB 48, 3156 (1993)

1. Introduction and theoretical foundation

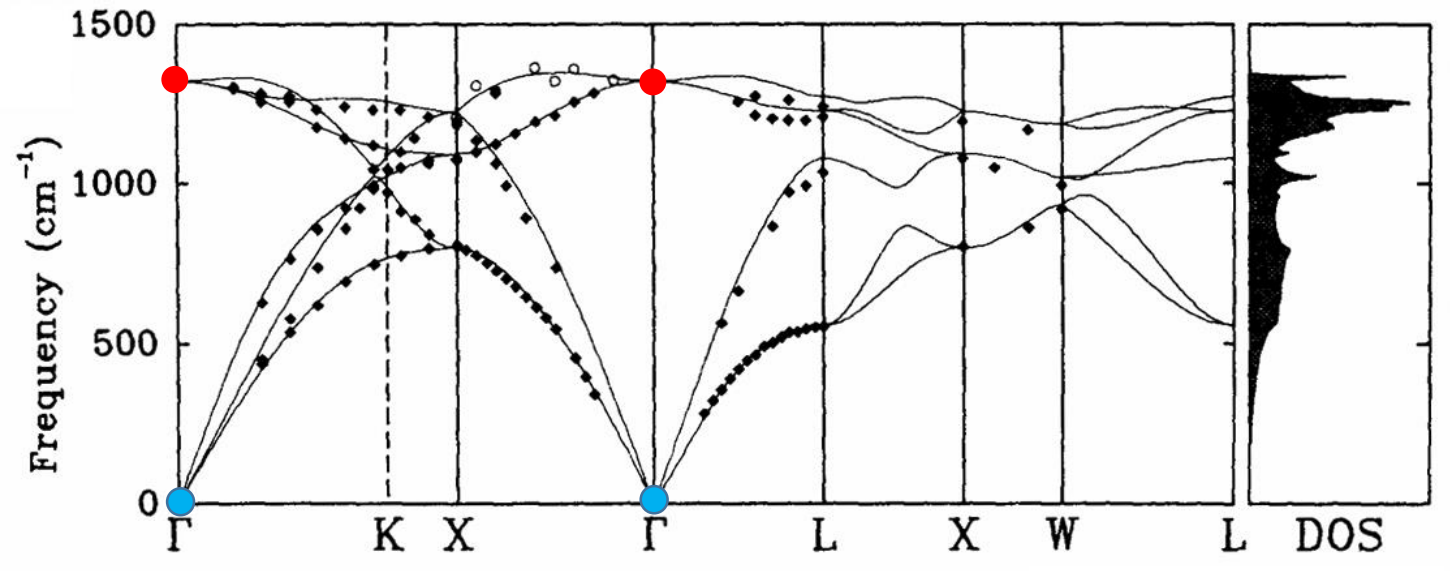

Brillouin light scattering

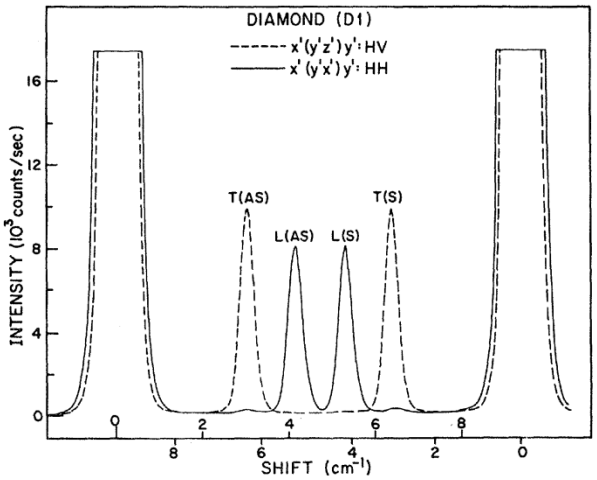

Raman scattering

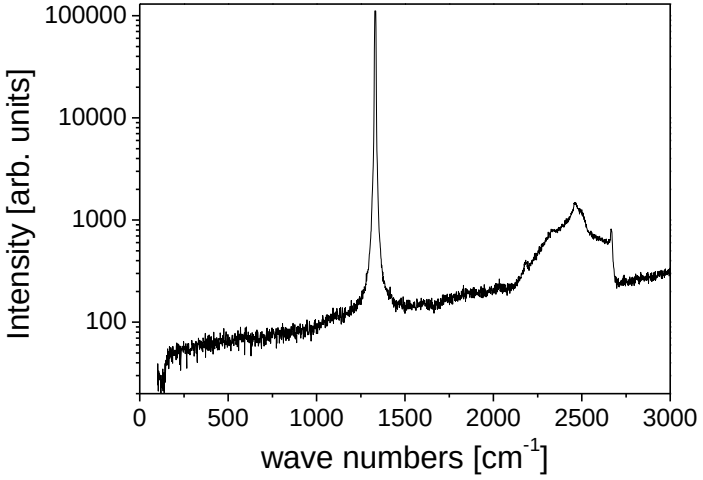

Information derived from IXS data

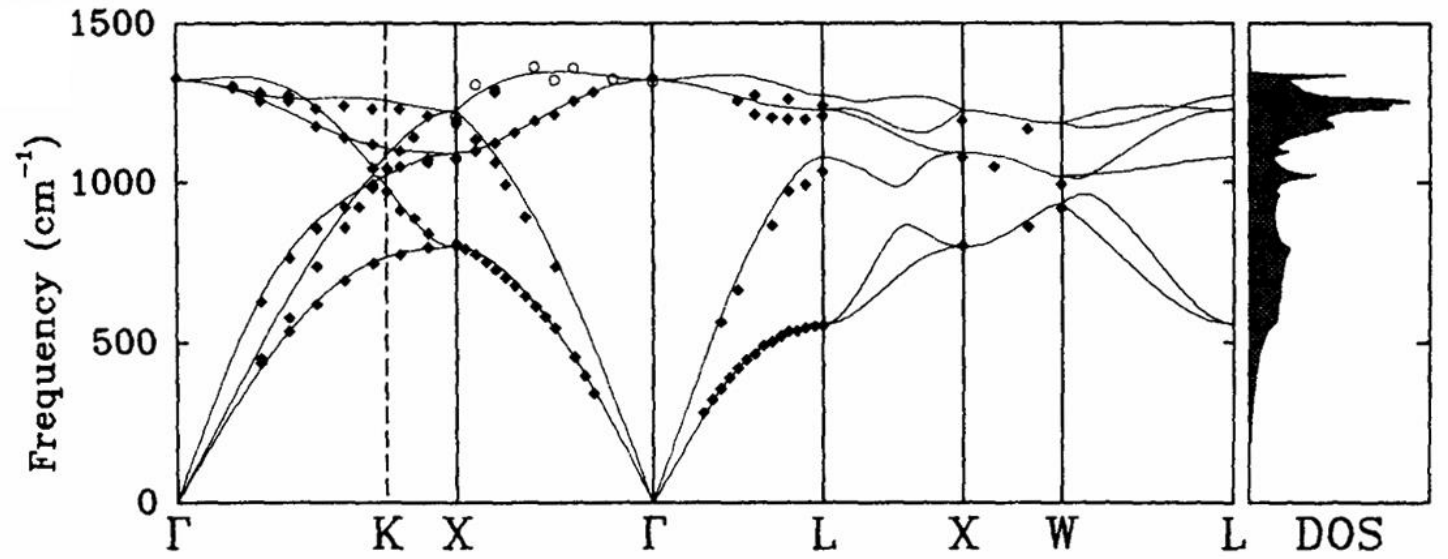

- Sound velocities
- Elasticity
- Interatomic force constants (potential)

- Dynamical instabilities (phonon softening)
- Anharmonicity
- Phonon-electron coupling

- Thermodynamics (C_V, S_V, θ_D, …)

X-rays and phonon studies?

Two citations from standard text books

"When a crystal is irradiated with X-rays, the processes of photoelectric absorption and fluorescence are no doubt accompanied by absorption and emission of phonons. The energy changes involved are however so large compared with phonon energies that information about the phonon spectrum of the crystal cannot be obtained in this way."

W. Cochran in Dynamics of atoms in crystals, (1973)

"…In general the resolution of such minute photon frequency is so difficult that one can only measure the total scattered radiation of all frequencies, … As a result of these considerations x-ray scattering is a far less powerful probe of the phonon spectrum than neutron scattering. "

Ashcroft and Mermin in Solid State Physics, (1975)

Vibrational spectroscopy: historical insight

Infrared absorption - 1881
W. Abney and E. Festing, R. Phil. Trans. Roy. Soc. 172, 887 (1881)

Brillouin light scattering - 1922
L. Brillouin, Ann. Phys. (Paris) 17, 88 (1922)

Raman scattering – 1928
C. V. Raman and K. S. Krishnan, Nature 121, 501 (1928)

TDS: Phonon dispersion in Al – 1948
P. Olmer, Acta Cryst. 1 (1948) 57

INS: Phonon dispersion in Al – 1955
B.N. Brockhouse and A.T. Stewart, Phys. Rev. 100, 756 (1955)

IXS: Phonon dispersion in Be – 1987
B. Dorner, E. Burkel, Th. Illini and J. Peisl, Z. Phys. B – Cond. Matt. 69, 179 (1987)

NIS: Phonon DOS in Fe – 1995
M. Seto, Y. Yoda, S. Kikuta, X.W. Zhang and M. Ando, Phys. Rev. Lett. 74, 3828 (1995)

1987 – first IXS measurements

Z. Phys. B – Condensed Matter 69, 179–183 (1987)

Condensed Matter
Zeitschrift für Physik B

First Measurement of a Phonon Dispersion Curve by Inelastic X-ray Scattering

B. Dorner*, E. Burkel, Th. Illini, and J. Peisl
Sektion Physik der Ludwig Maximilians Universität, München, Federal Republic of Germany

Received July 6, 1987

Inelastic scattering of 13.8 keV X-rays with very high energy resolution of $\Delta E = 55$ meV was used to measure the phonon dispersion curves for the *LA* and *LO* modes in the [00ξ] direction in Be. The results agree with inelastic neutron scattering data known from the literature. The X-ray scattering intensities of the phonon excitations for different momentum transfers are in very good agreement with the prediction from the scattering law.

HASYLAB

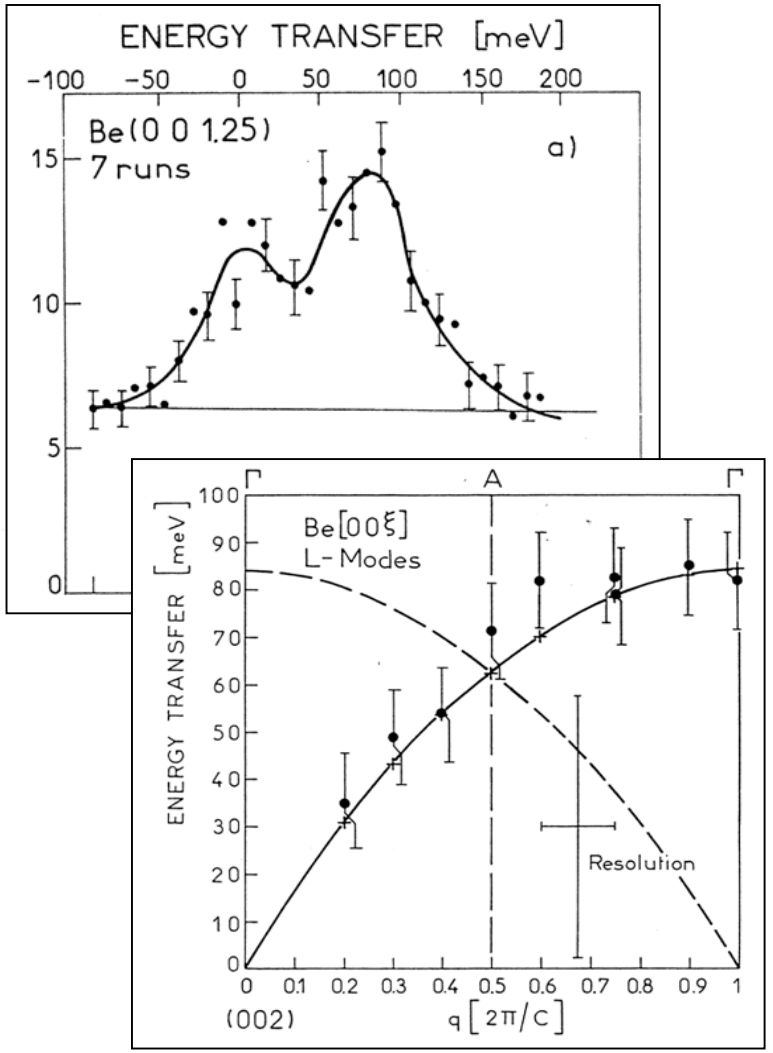

Inelastic Scattering from Phonons

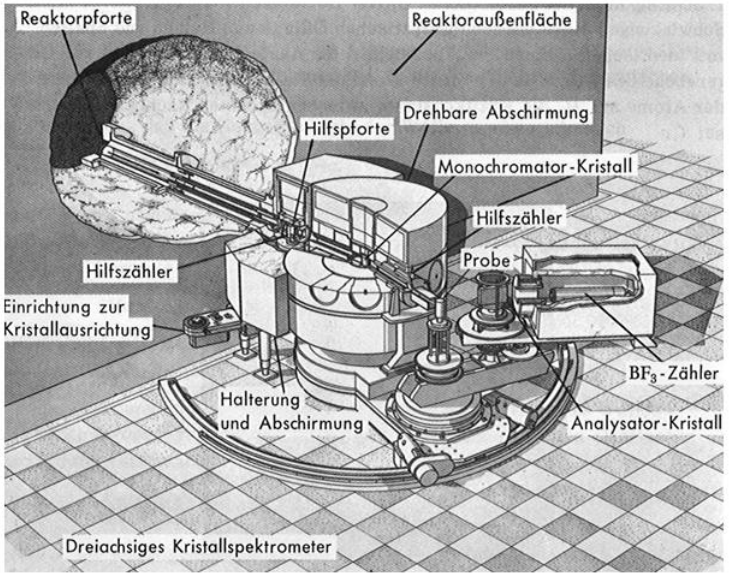

Brockhouse (1955)

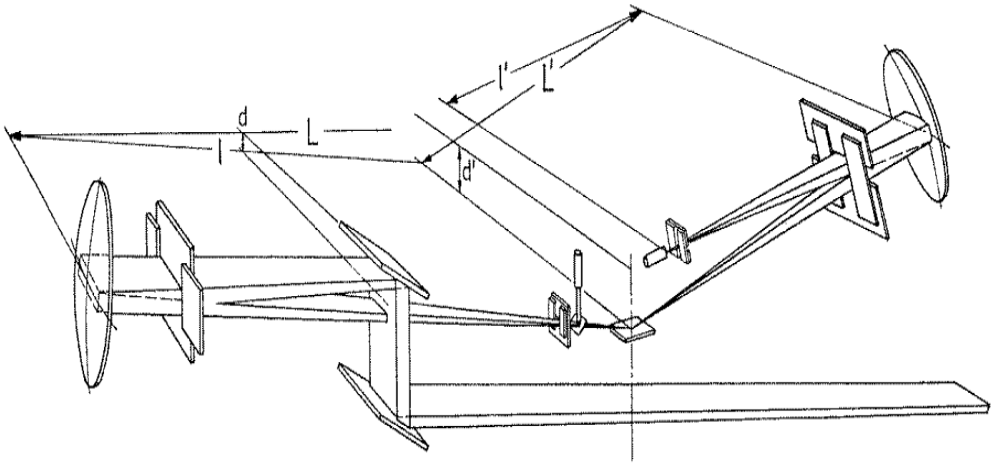

The instrument INELAX at the HARWI wiggler line of HASYLAB.

Burkel, Dorner and Peisl (1987)

Thermal neutrons:

E_i = 25 meV

k_i = 38.5 nm^{-1}

$\Delta E/E$ = 0.01 – 0.1

Hard X-rays:

E_i = 18 keV

k_i = 91.2 nm^{-1}

$\Delta E/E \leq 1x10^{-7}$

IXS versus INS

IXS

$$\frac{\partial^2\sigma}{\partial E\partial\Omega} = r_0^2 \frac{k_1}{k_2}(\vec{\varepsilon}_1 \cdot \vec{\varepsilon}_2) f(Q)^2 \, S(\vec{Q}, E)$$

- no correlation between momentum- and energy transfer
- $\Delta E/E = 10^{-7}$ to 10^{-8}
- Cross section ~ Z^2 (for small Q)
- Cross section is dominated by photoelectric absorption (~ $\lambda^3 Z^4$)
- no incoherent scattering
- small beams: 10 μm or smaller

INS

$$\frac{\partial^2\sigma}{\partial E\partial\Omega} = b^2 \frac{k_1}{k_2} S(\vec{Q}, E)$$

- strong correlation between momentum- and energy transfer
- $\Delta E/E = 10^{-1}$ to 10^{-2}
- Cross section ~ b^2
- Weak absorption => multiple scattering
- incoherent scattering contributions
- large beams: several cm

Scientific themes

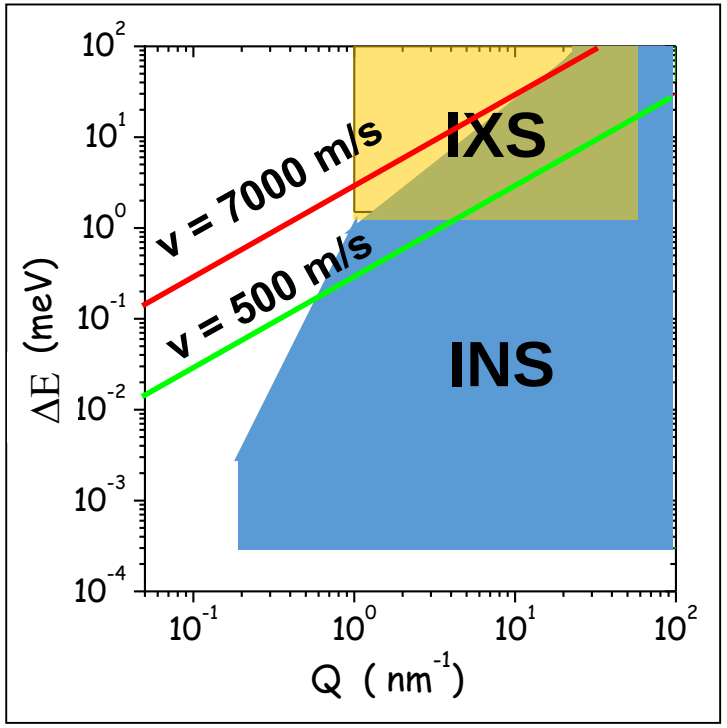

Disordered systems, small crystals

$$Q = 4\pi/\lambda \cdot \sin(\theta/2)$$
$$\Delta E = E_i - E_f$$

- Phonons in crystalline materials
- Interplay between structure and dynamics
- Relaxations on the picosecond time scale
- Nature of sound propagation and attenuation

Small sample volumes: 10^{-4} – 10^{-5} mm^3

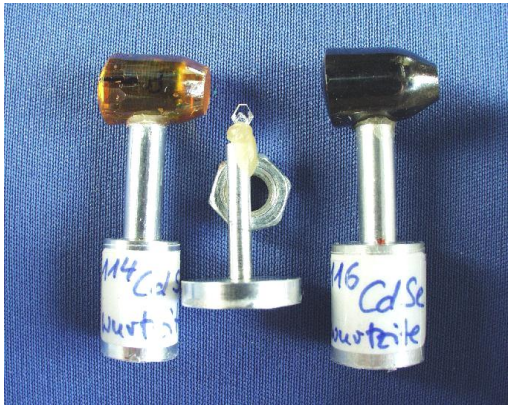

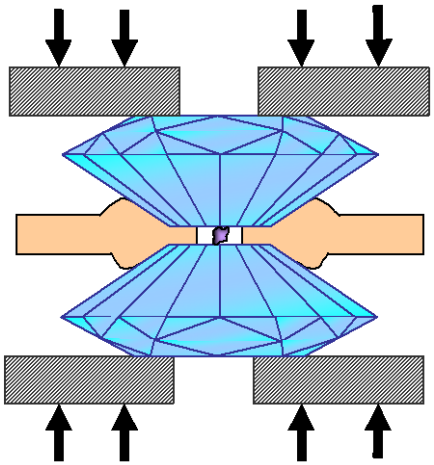

Diamond anvil cell

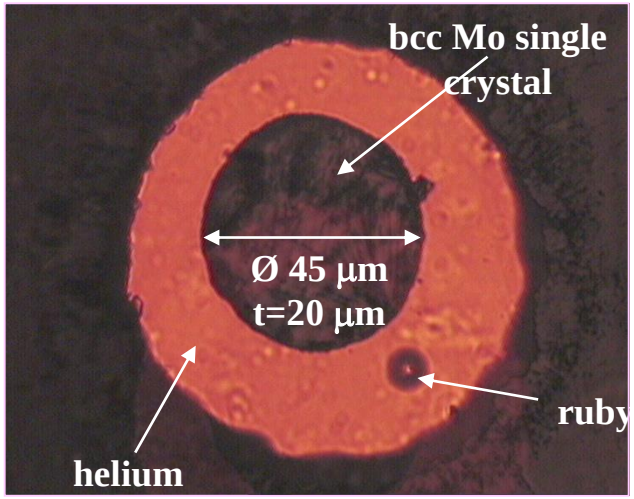

- (New) materials in very small quantities
- Very high pressures > 1Mbar
- Study of surface phenomena

High resolution IXS: instrumentation

ESRF: a European collaboration

The ESRF is financed by 19 countries.

Experimental IXS set-up

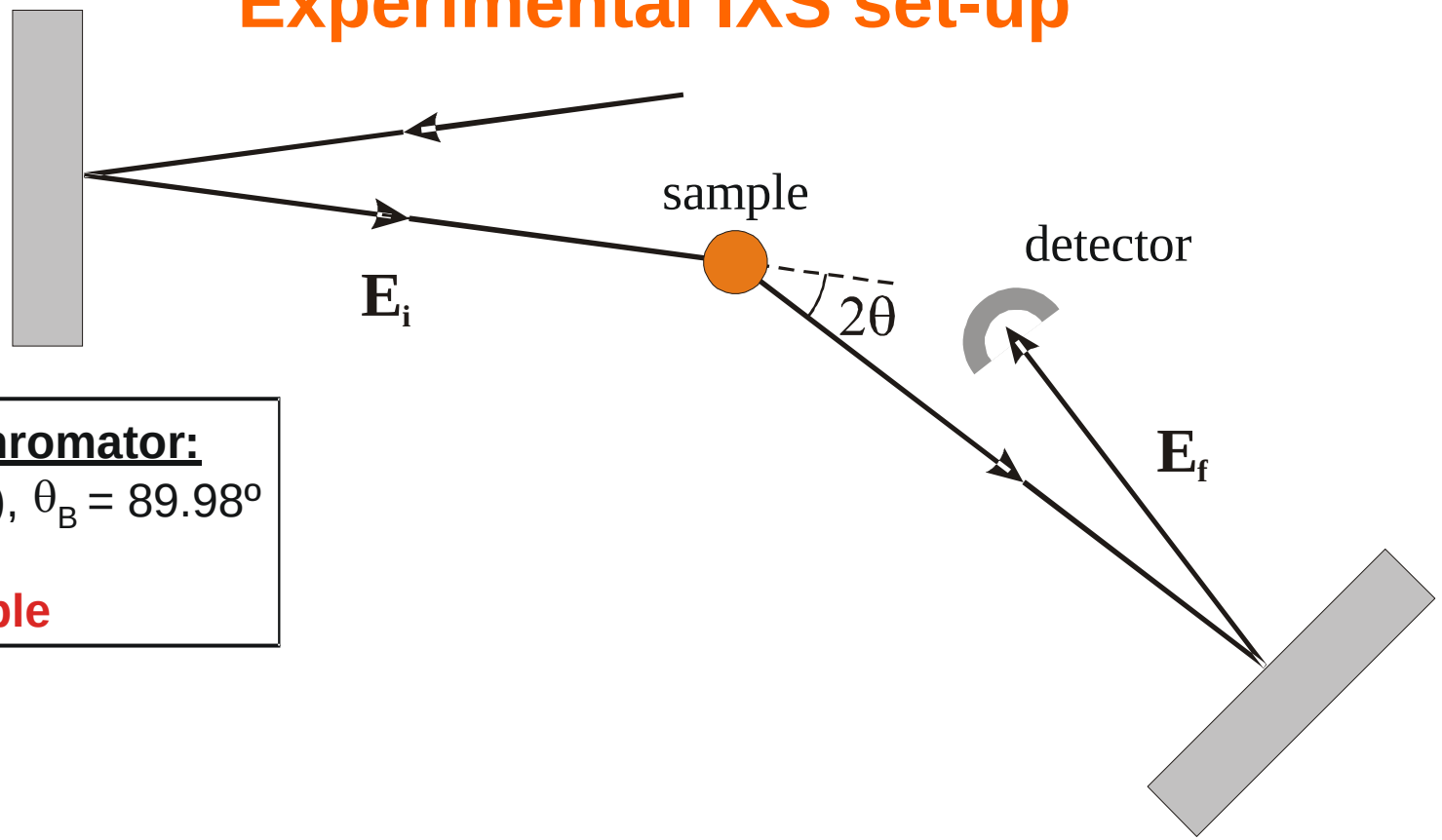

Monochromator:
Si(n,n,n), θ_B = 89.98º
n=7-13
λ_1 **tunable**

Spot size: 30 x 60 μm^2 (H x V)

Analyser:
Si(n,n,n), θ_B = 89.98º
n=7-13
λ_2 **constant**

IXS set-up: energy scanning

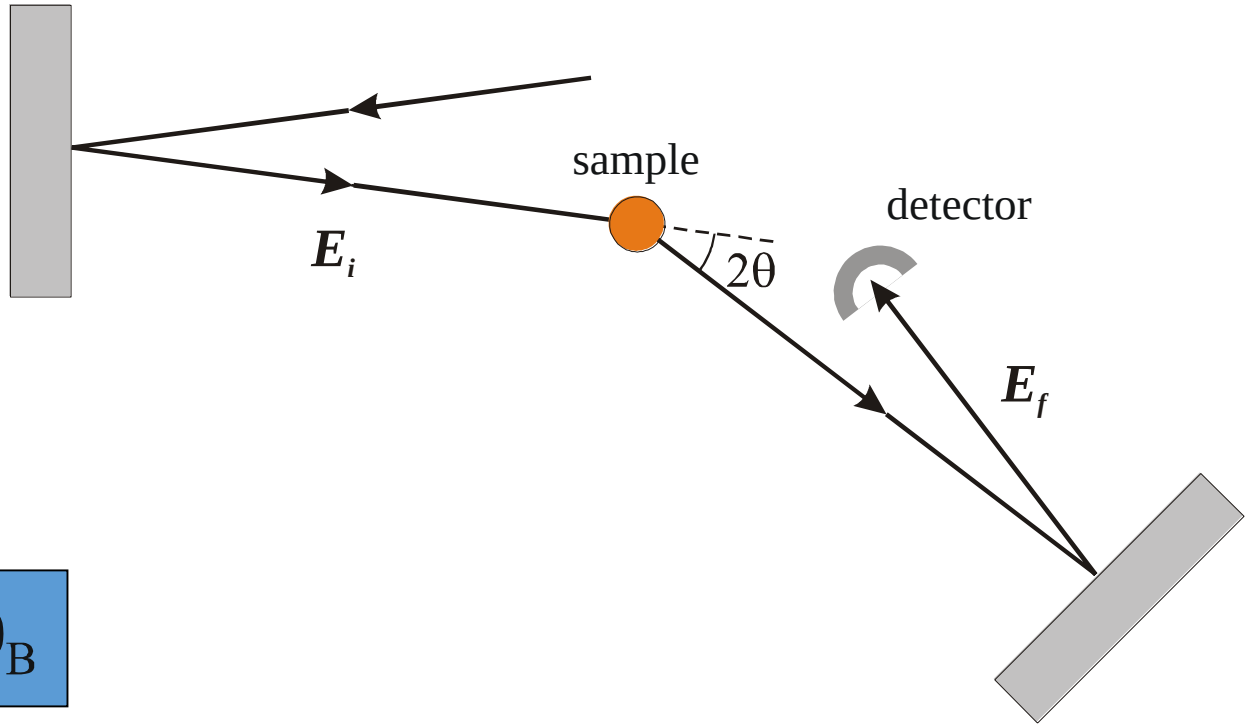

$$\mathbf{Q} = 4\pi/\lambda \cdot \sin(\theta)$$

$$\lambda = 2 \cdot d(T) \sin\theta_B$$

$$\Delta d/d = \Delta \mathbf{E}/E = -\alpha(T) \cdot \Delta T \ (\alpha = 2.58 \cdot 10^{-6} \text{ at RT})$$

ID28 at the ESRF beamline layout

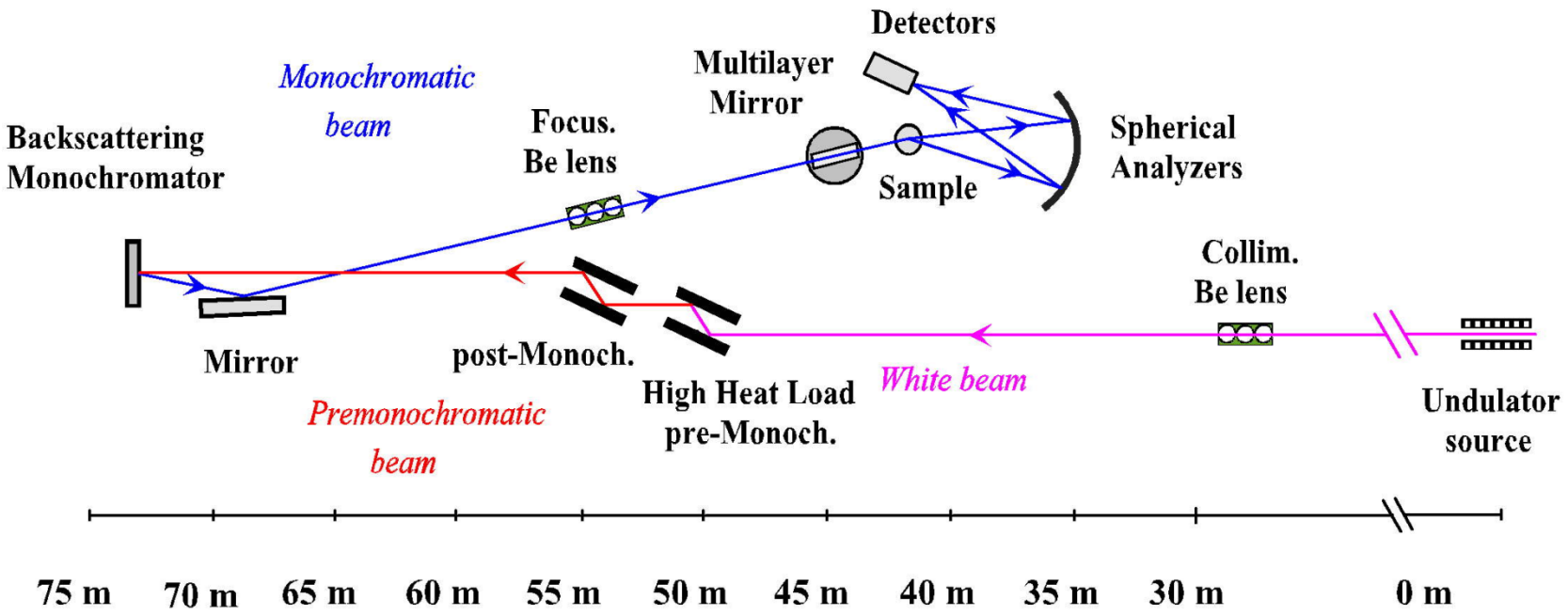

Main monochromator

AIM:

- Reduce the bandwidth from ~$1 \cdot 10^{-4}$ to 10^{-7}-10^{-8}
- Accept the whole beam (V-divergence: 20 μrad)

SOLUTION:

Backscattering crystal operating at high reflection order

Si(n n n) Reflection	E [eV]	ΔE [meV]	ΔE/E	3 x U35 flux [photons/s]
7	13839	5.3	$3.8 \cdot 10^{-7}$	$1.0 \cdot 10^{-11}$
8	15816	4.4	$2.8 \cdot 10^{-7}$	$7.6 \cdot 10^{-10}$
9	17793	2.2	$1.2 \cdot 10^{-7}$	$2.4 \cdot 10^{-10}$
11	21747	0.83	$4.7 \cdot 10^{-8}$	$4.6 \cdot 10^{-9}$
12	23724	0.73	$3.1 \cdot 10^{-8}$	$3.4 \cdot 10^{-9}$
13	25701	0.5	$1.9 \cdot 10^{-8}$	$1.0 \cdot 10^{-9}$

ϑ_B=89.98°, α=85°

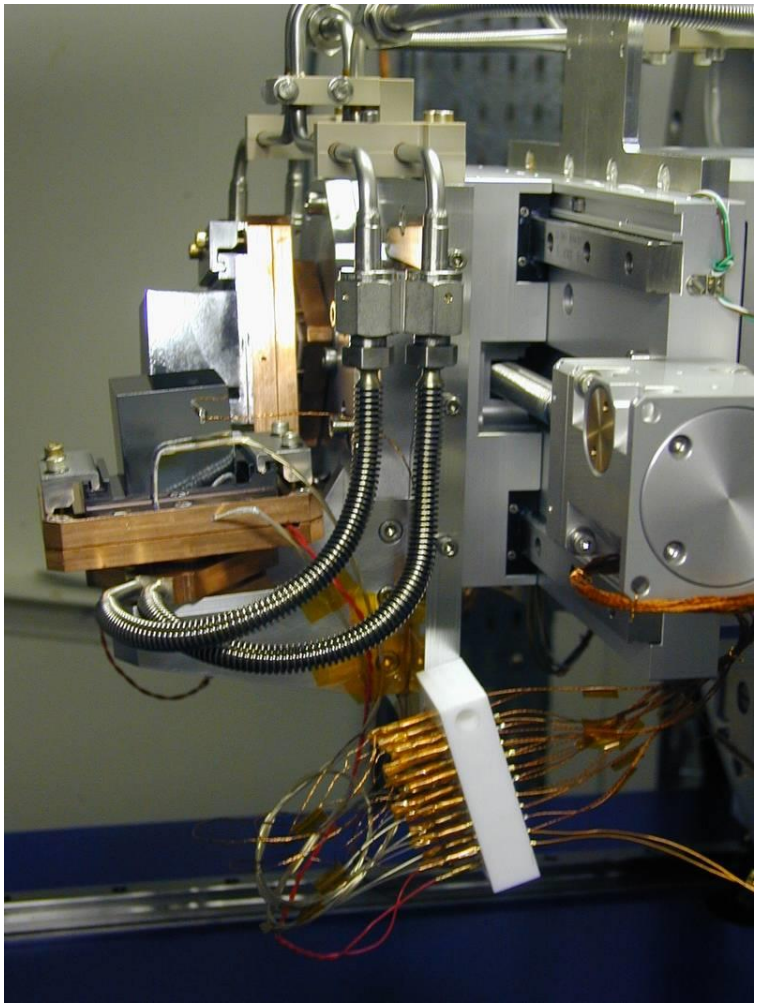

High-resolution spectrometer

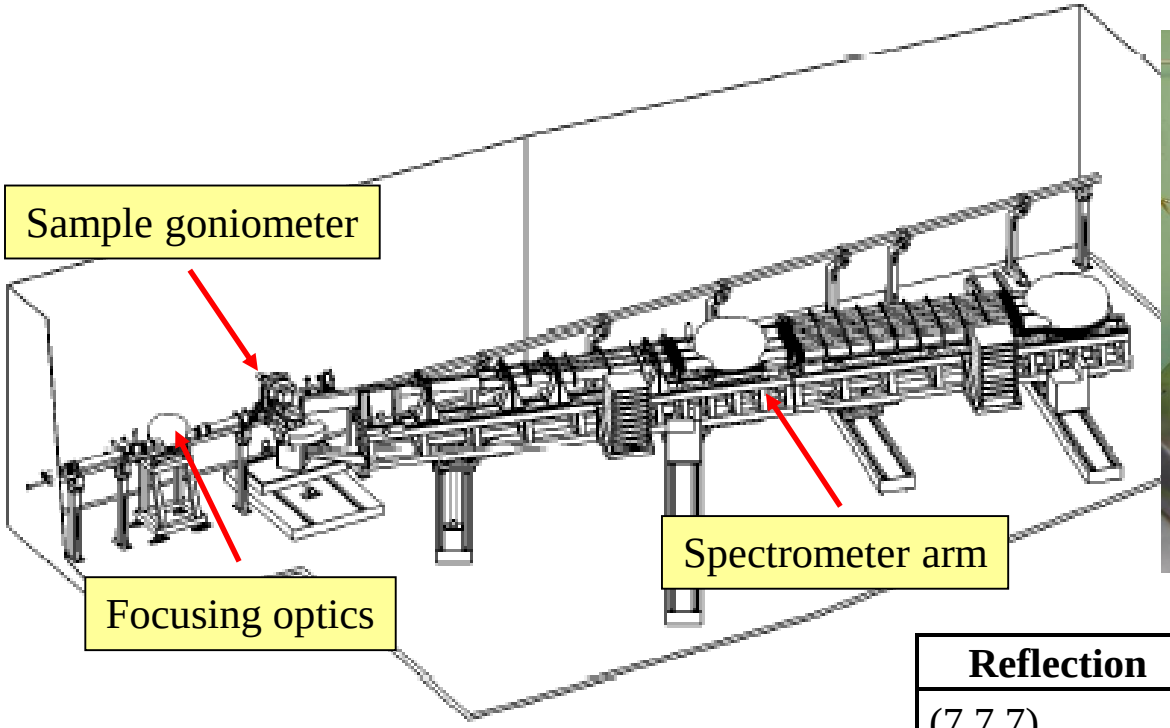

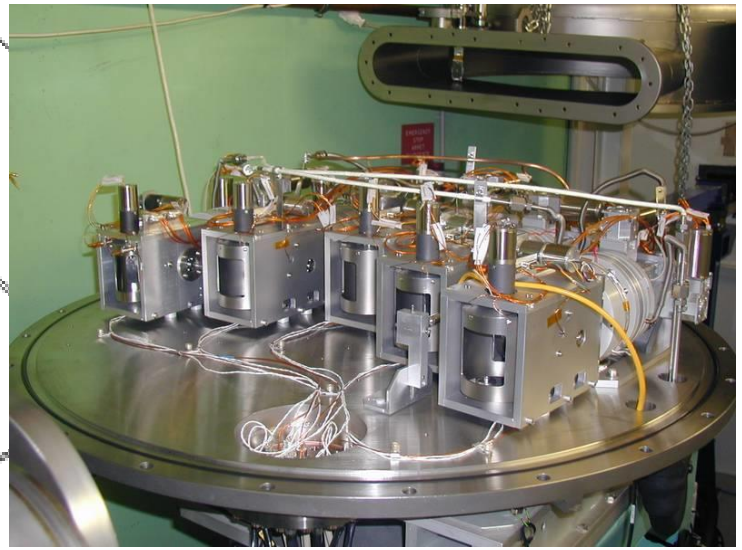

Reflection	ΔE [meV]	$Q_{max}(7)$ [nm^{-1}]
(7 7 7)	7	64
(8 8 8)	5.5	73
(9 9 9)	3.0	82
(11 11 11)	1.7	100
(13 13 13)	0.9	119

Spectrometer: analysers and detector

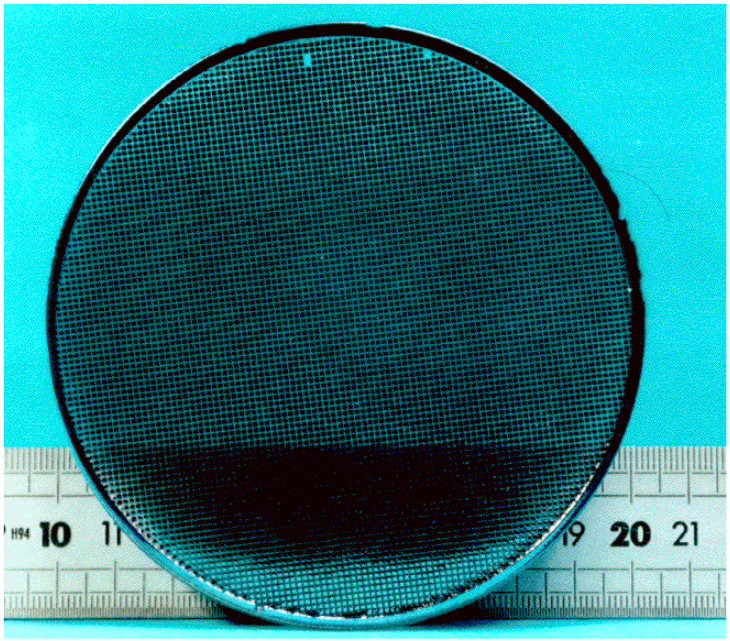

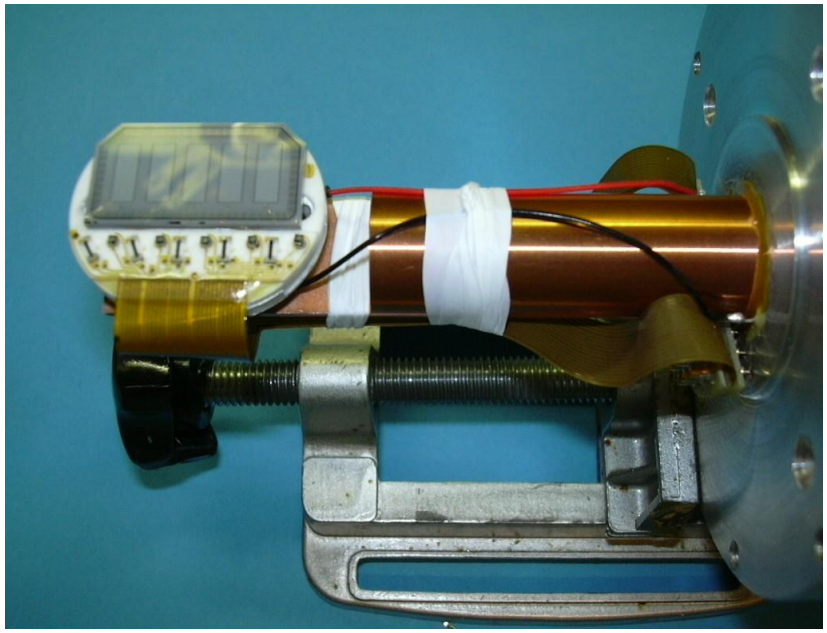

- ~10.000 cubes of 0.6x0.6x2.3 mm^3
- perfect crystal properties
- collection of sufficient solid angle

- 5 x 1.5 mm Si diodes at 20° incidence
- 1 count/20'
- Canberra – Eurisys
- Signal loss: 4% (15%) at n=11 (n=13)

High-resolution IXS: examples of applications

Phonon dispersion of fcc d-Plutonium

Pu is one of the most fascinating and exotic element known

- Multitude of unusual properties
- Central role of 5f electrons
- Radioactive and highly toxic

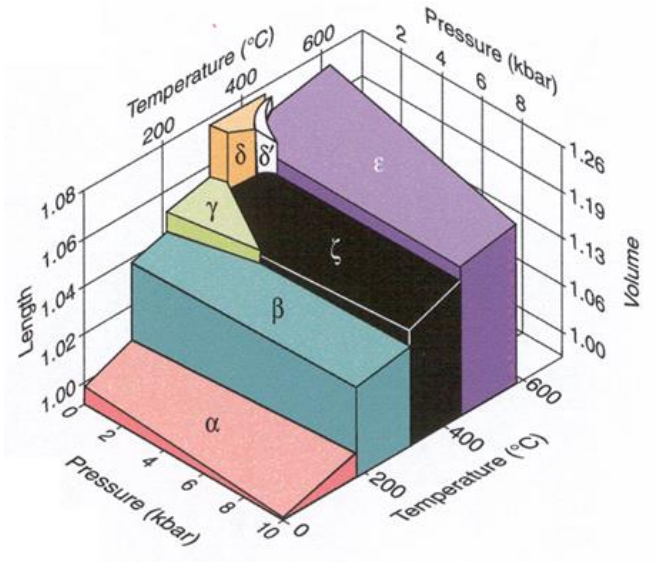

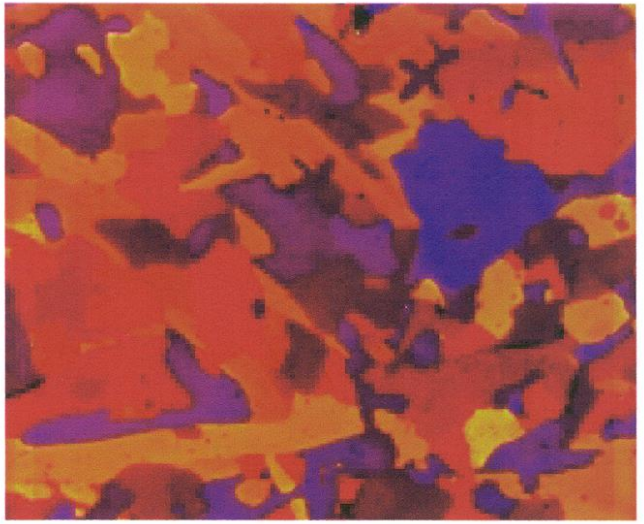

strain enhanced recrystallisation of fcc Pu-Ga (0.6 wt%) alloy

typical grain size: **90 μm**
foil thickness: **10 μm**

Wong et al. Science 301, 1078 (2003); PRB 72, 064115 (2005)

Plutonium: The IXS experiment

- Energy resolution: 1.8 meV at 21.747 keV
- Beam size: 20 x 60 μm^2 (FWHM)
- On-line diffraction analysis

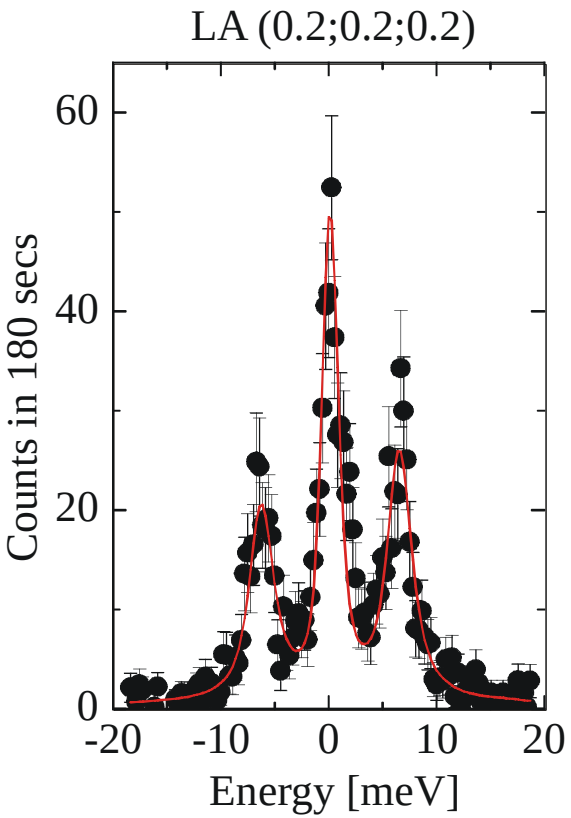

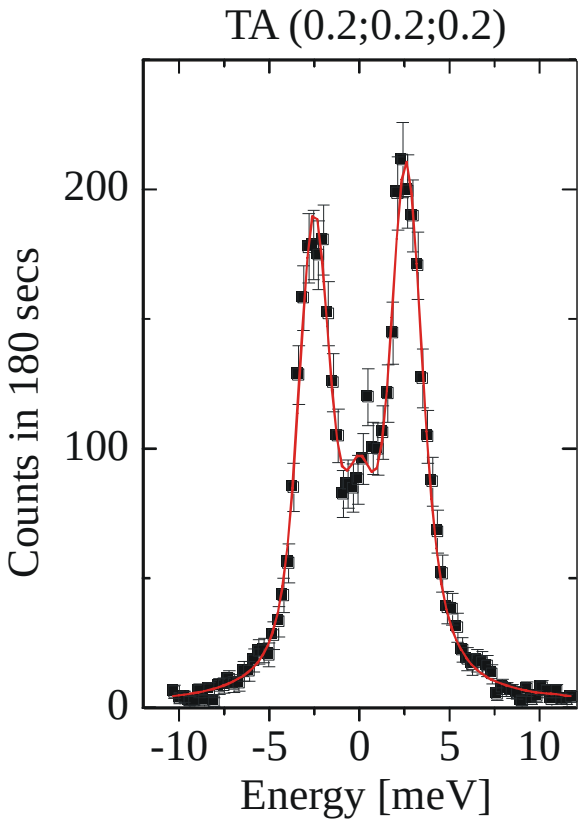

Plutonium: phonon dispersion

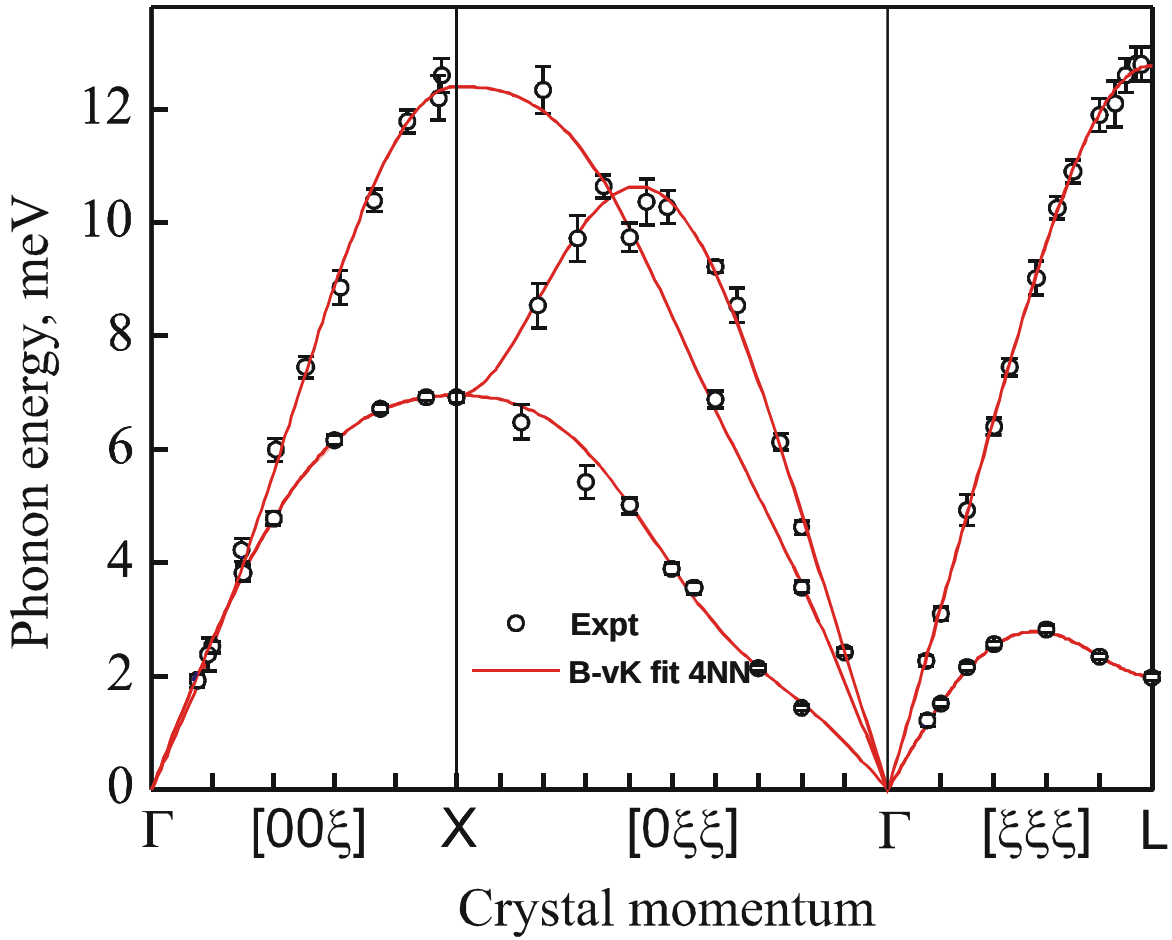

- **Born-von Karman force constant model fit**

- good convergence, if fourth nearest neighbors are included

Plutonium: elasticity

Proximity of Γ-point: E = Vq

$V_L[100] = (C_{11}/\rho)^{1/2}$

$V_T[100] = (C_{44}/\rho)^{1/2}$

$V_L[110] = ([C_{11}+C_{12}+2C_{44}]/\rho)^{1/2}$

$V_{T1}[110] = ([C_{11} - C_{12}]/2\rho)^{1/2}$

$V_{T2}[110] = (C_{44}/\rho)^{1/2}$

$V_L[111] = [C_{11}+2C_{12}+4C_{44}]/3\rho)^{1/2}$

$V_T[111] = ([C_{11}-C_{12}+C_{44}]/3\rho)^{1/2}$

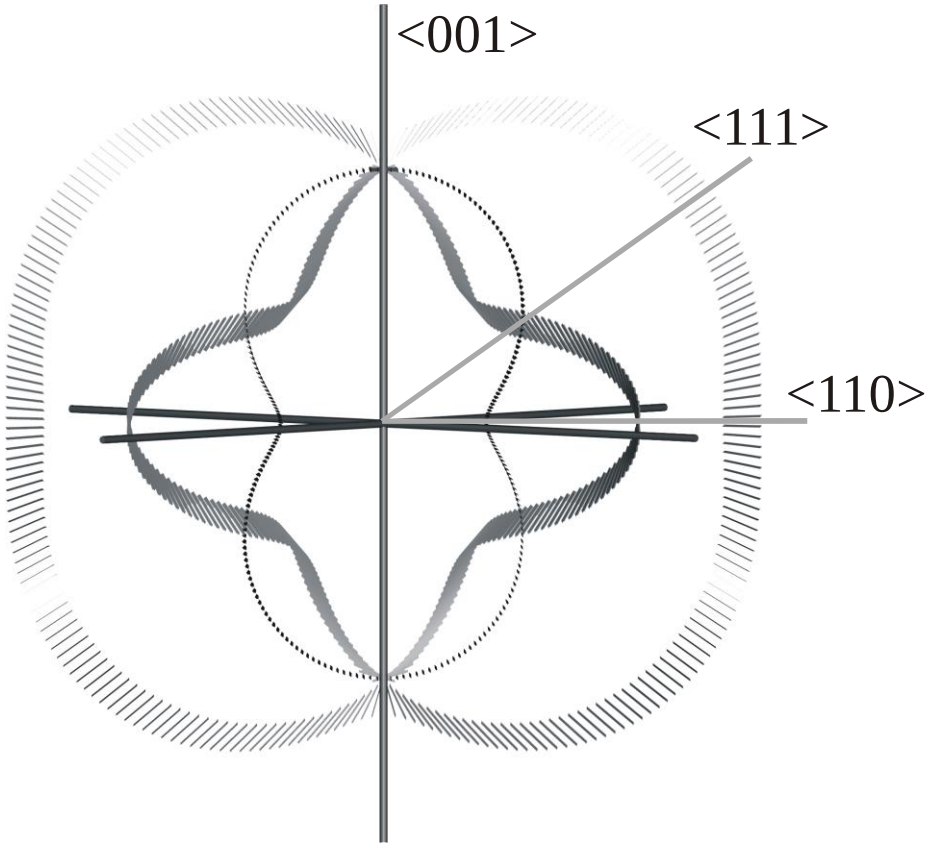

C_{11} = 35.3±1.4 GPa

C_{12} = 25.5±1.5 GPa

C_{44} = 30.5±1.1 GPa

highest elastic anisotropy
of all known fcc metals

Scattering from powders

phonon energy

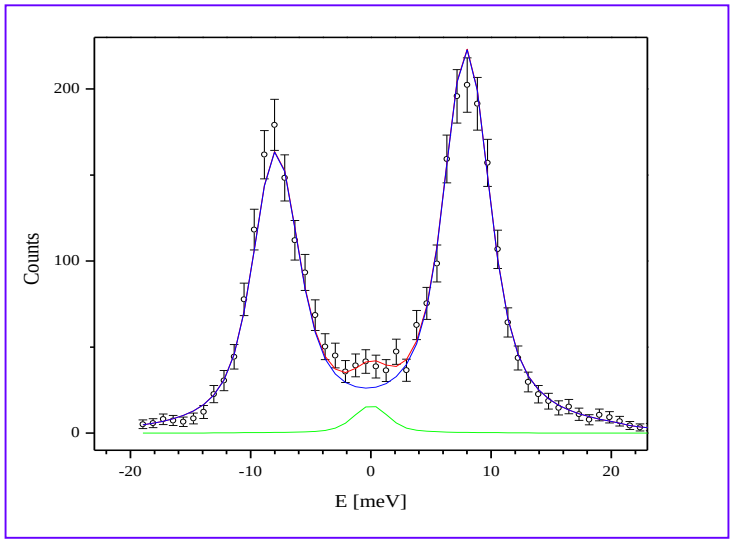

Phonon dispersion

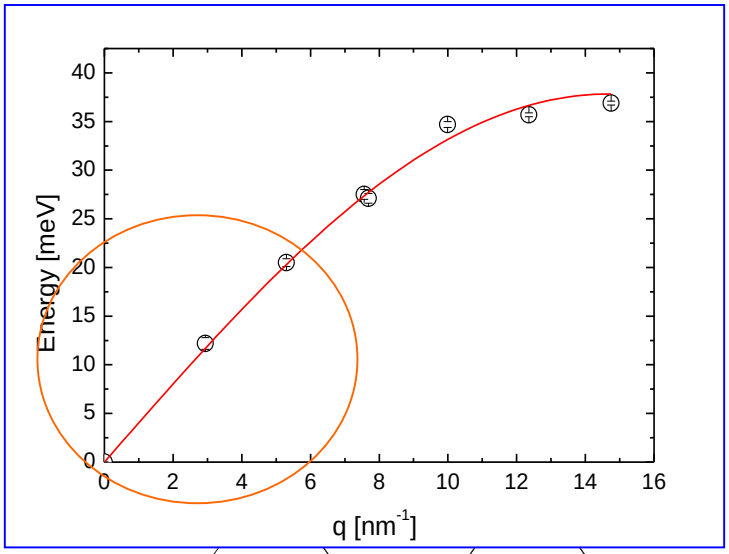

direction of momentum transfer is not defined:

integration over shell with radius |Q|

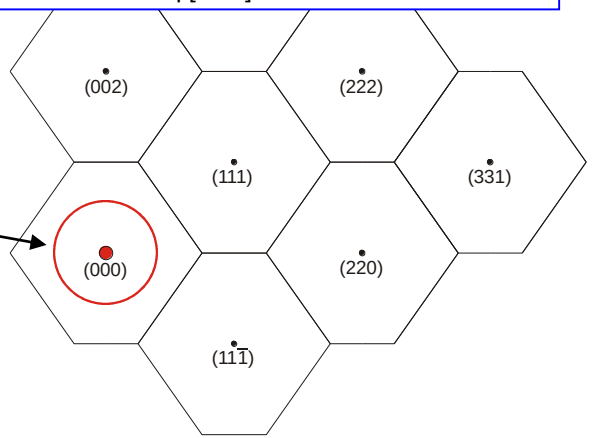

low Q – long-wave limit

orientational average of LA phonon energy linked to the elasticity

IXS from polycrystalline samples

Determination of orientation averaged properties

- aggregate sound velocities: V_L, (V_T)
- phonon density of states: V_D, C_V, Θ_D, …

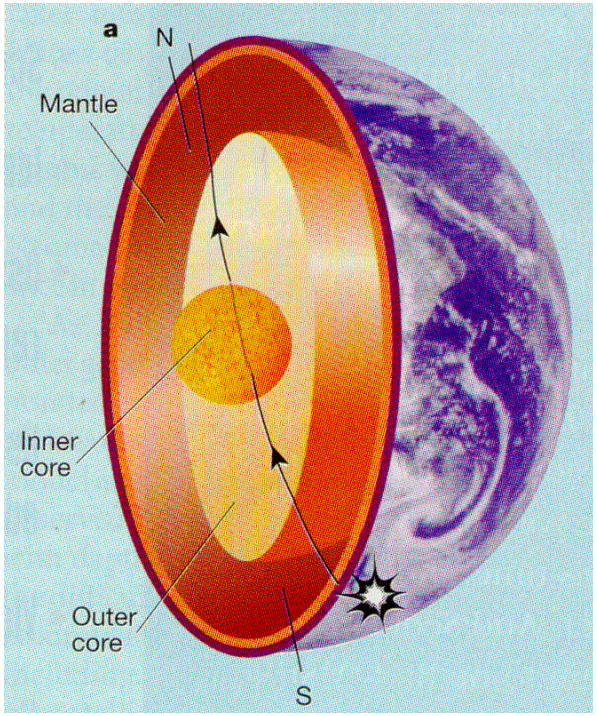

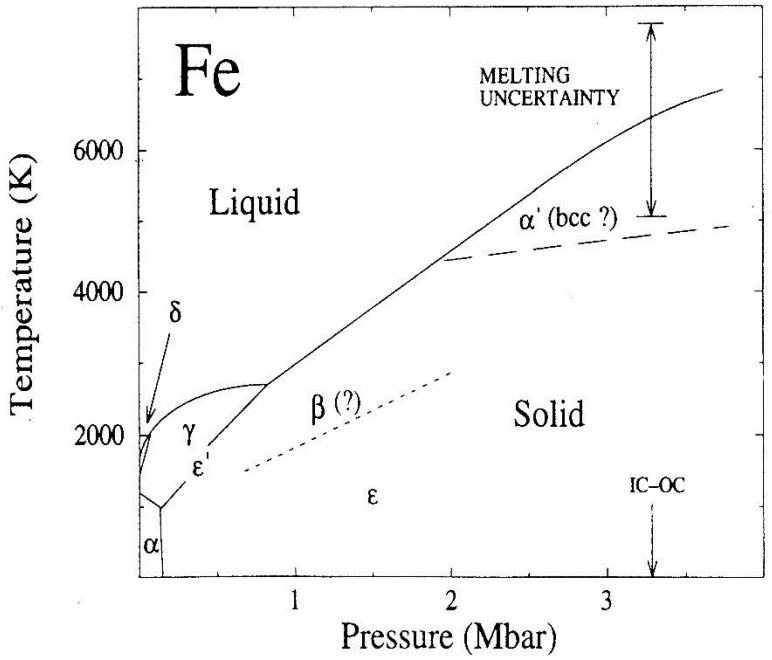

hcp iron: raw spectra and phonon dispersion

P =55 GPa

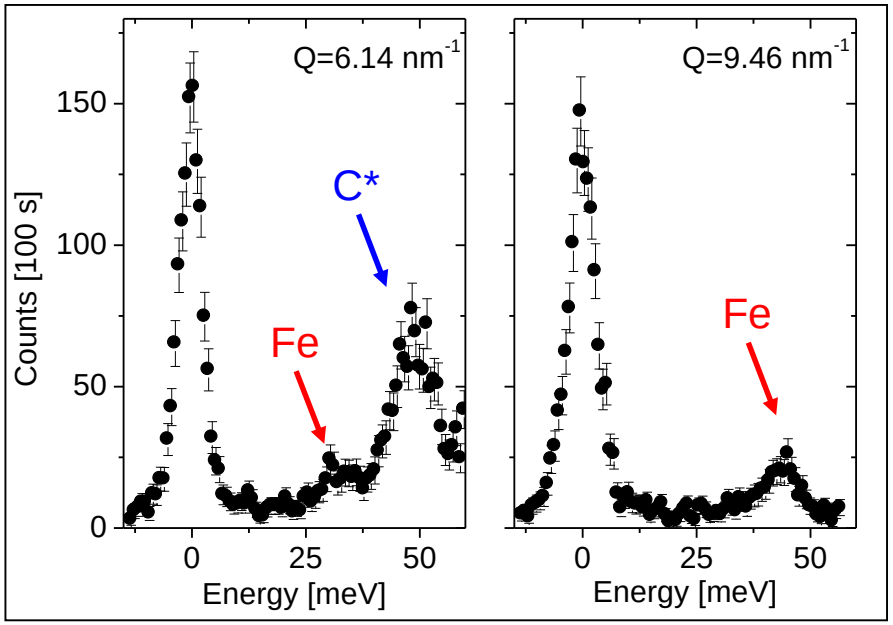

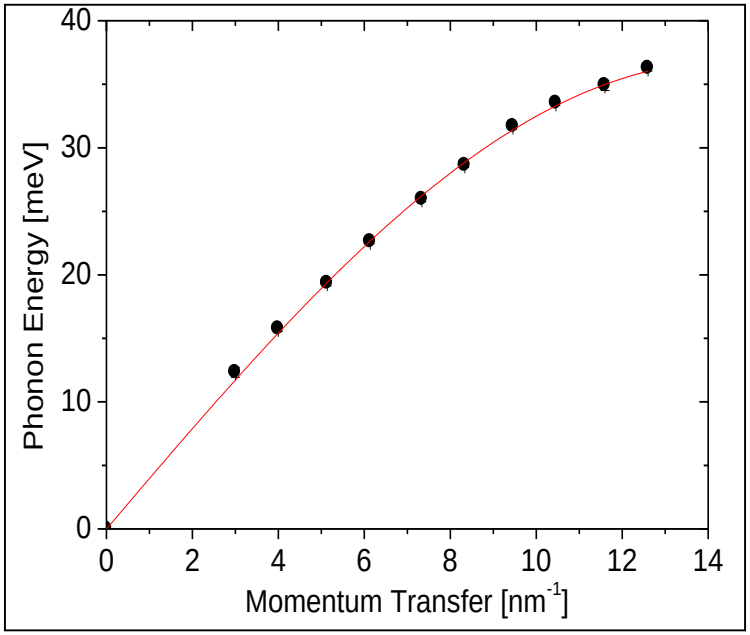

V_P from initial slope of dispersion curve via sine fit:

$$V_P = 1519 \cdot E\,[\mathrm{meV}]/Q[\mathrm{nm}^{-1}]$$

Density dependence of V_P and V_S

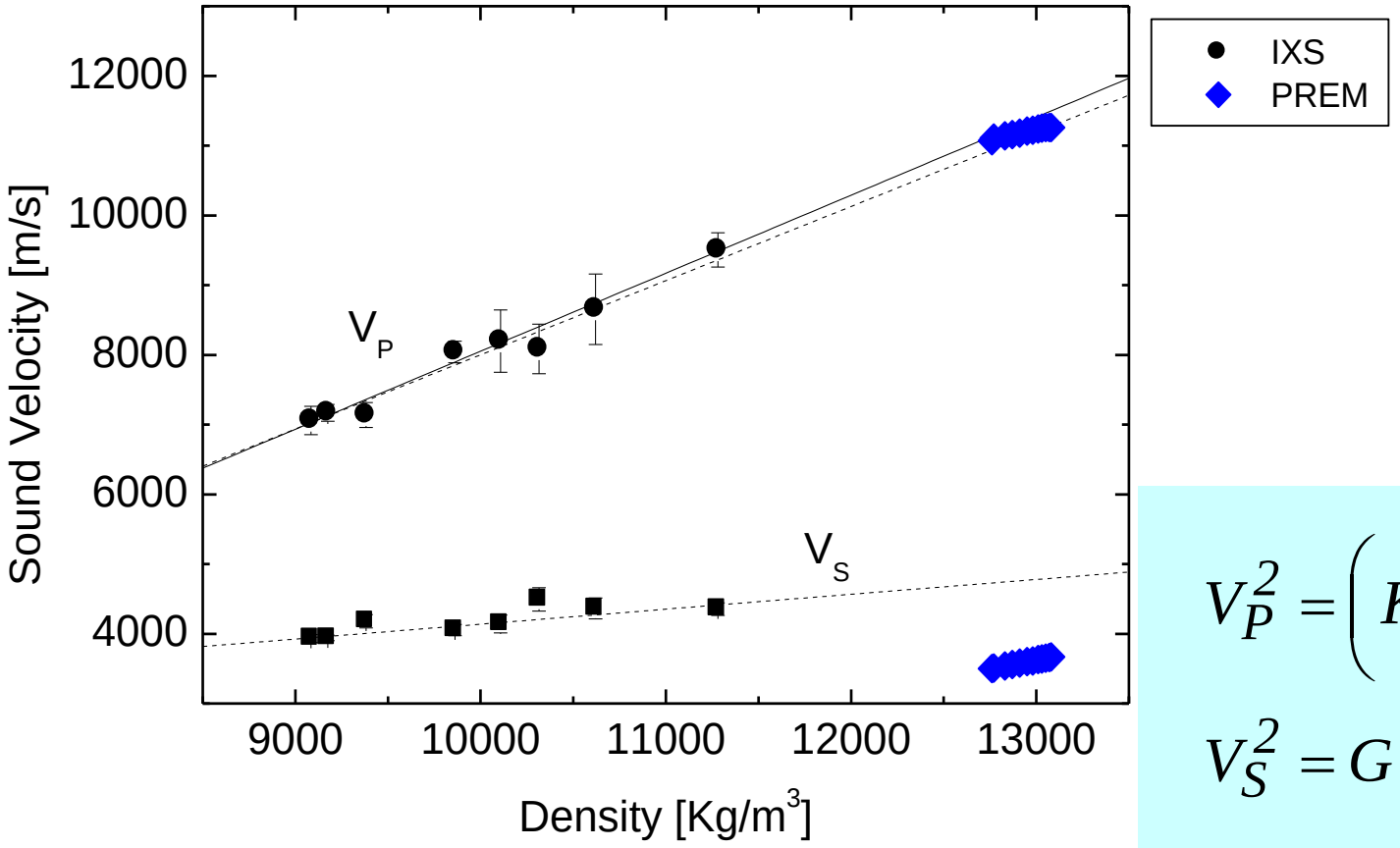

$$V_P^2 = \left(K + \frac{4}{3} G \right) / \rho$$

$$V_S^2 = G / \rho$$

Fiquet et al., Science 291, 468 (2001); Antonangeli et al., EPSL 225, 243 (2004)

The puzzle of the microscopic dynamics

Microscopic regime → not complete understanding

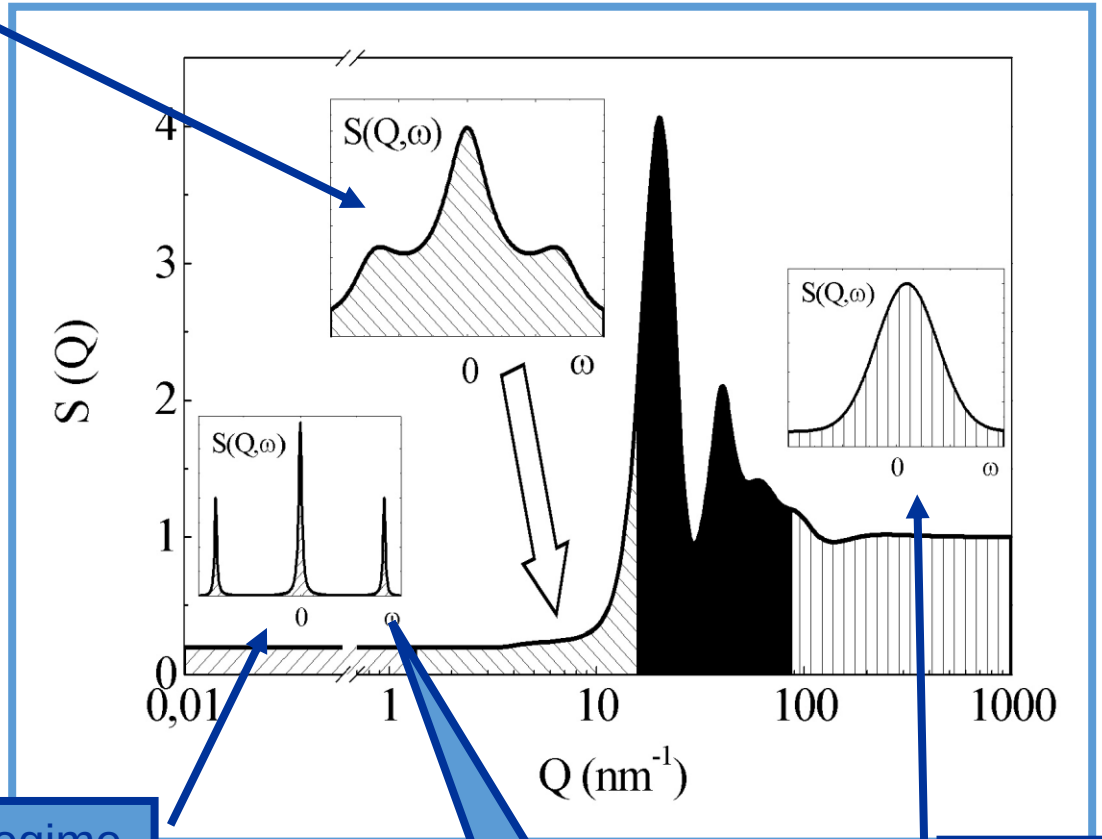

Macroscopic regime → hydrodynamics

v=ħω/q

Free particle regime: kinetic theory

Short range order in liquids

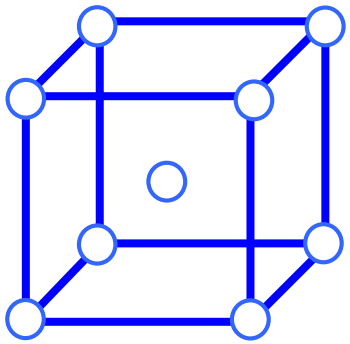

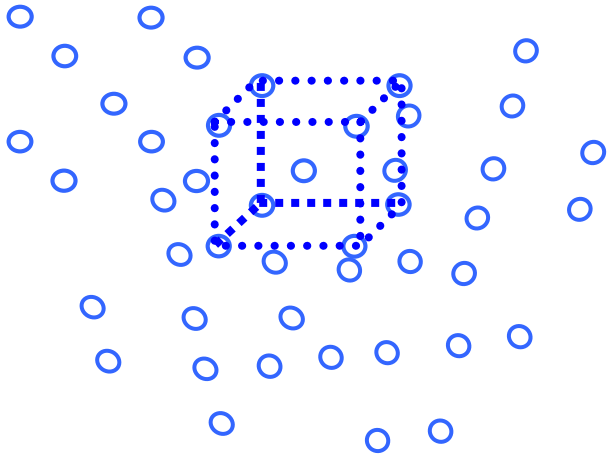

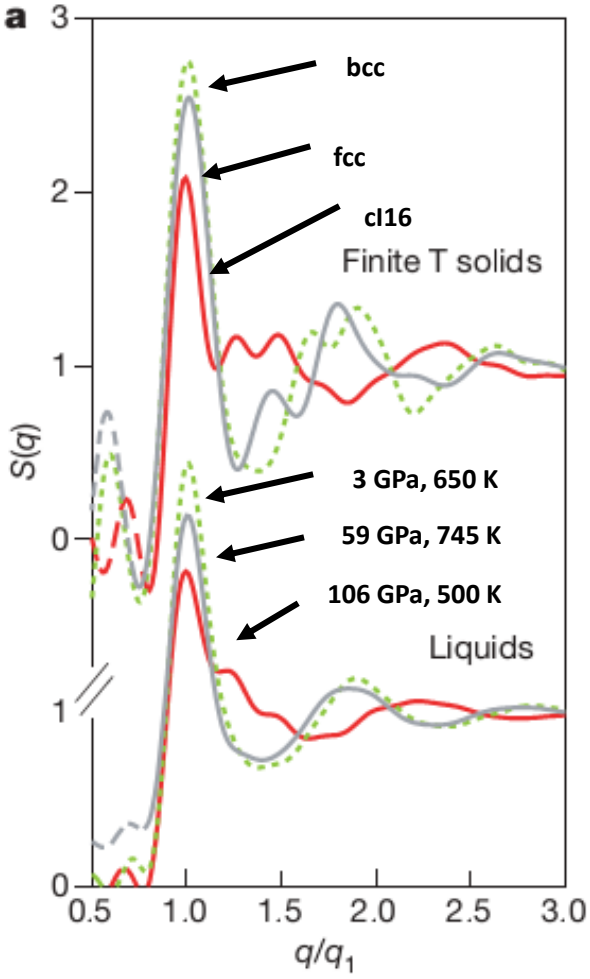

Es. sodium: the short range order of the liquid evolves with P and T following similar transformations as in the solid phase

Raty et al., Nature 449, 448 (07)

The dynamic structure factor of sodium

Inelastic x-ray scattering data @ ID16, E=23.724 keV, ΔE=1.4 meV

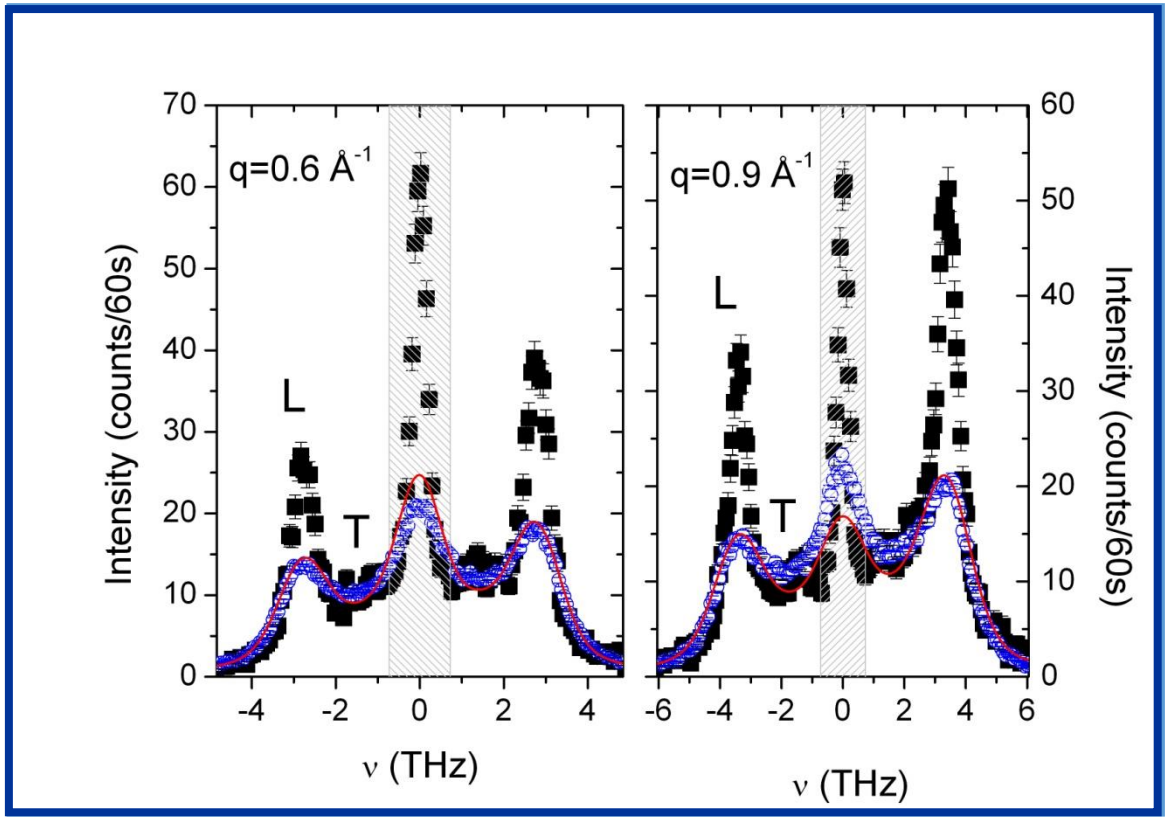

The spectrum of the liquid is a broadened version of the one for the (poly)crystal

Giordano & g.m., PNAS 107, 21985 (10)

The order fingerprint

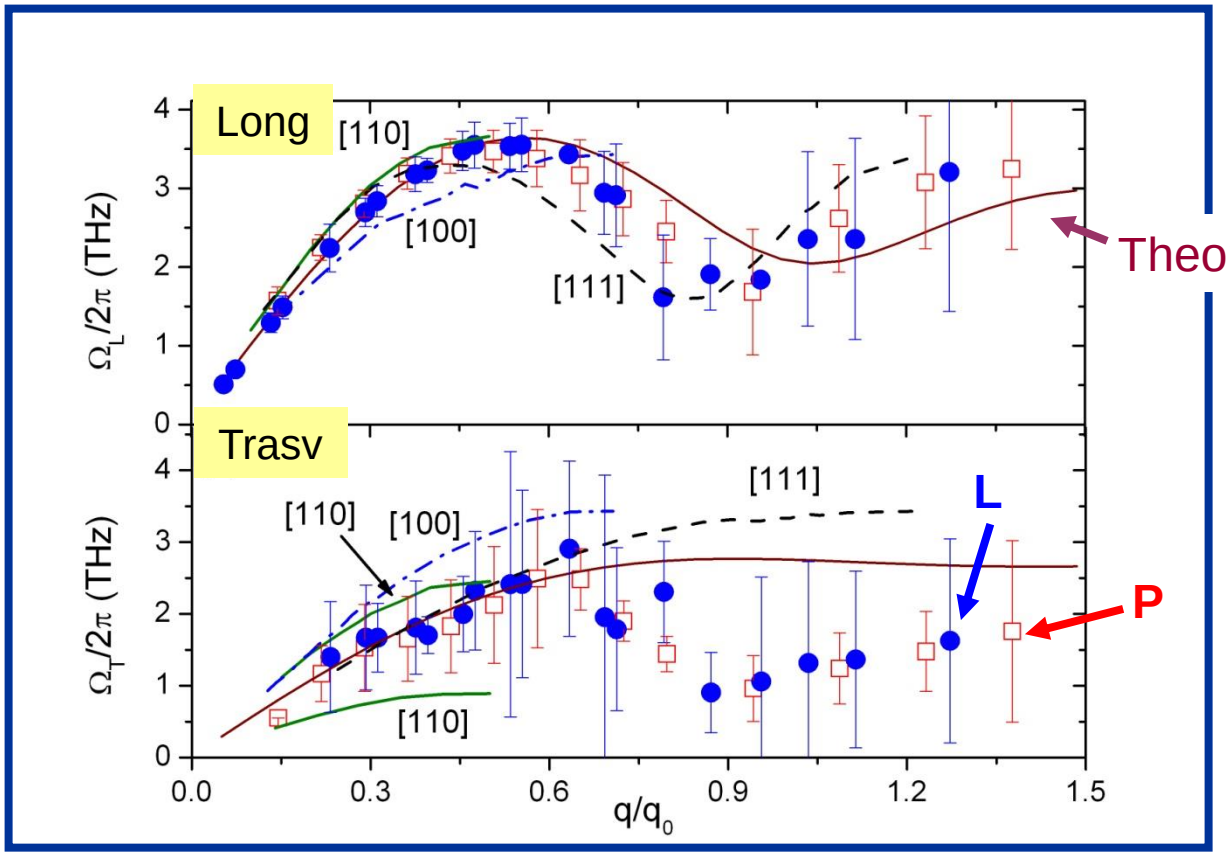

Giordano & g.m., PNAS 107, 21985 (10)

First Brillouin zone:

The longitudinal and transverse dispersion curves in the liquid reflect those for the polycrystal:
an orientational average over the high symmetry branches of the single crystal

(density scaling of frequencies for the solid)

The disorder fingerprint

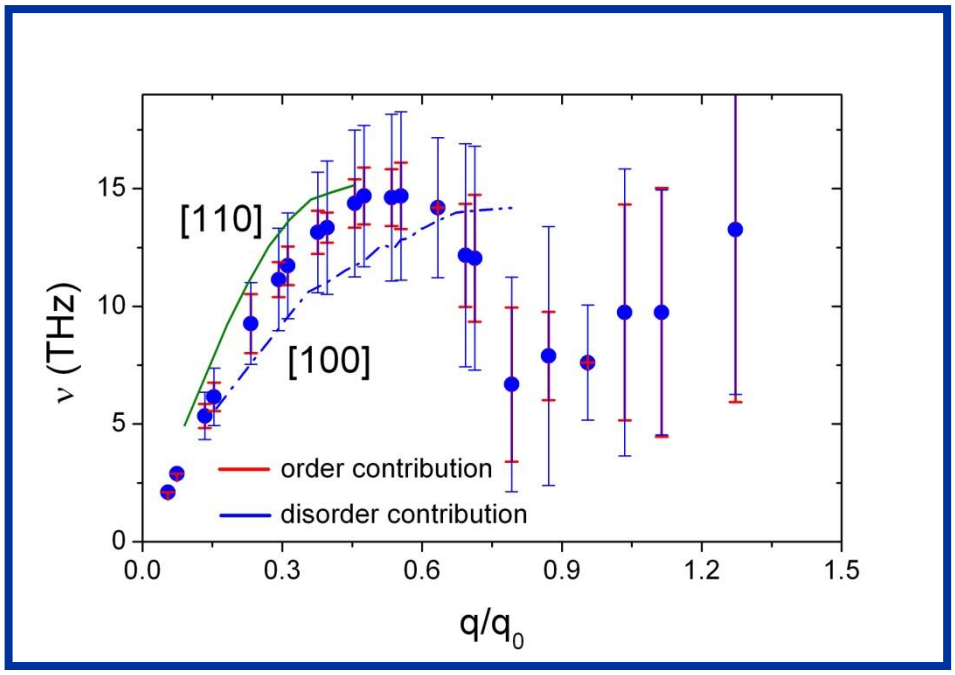

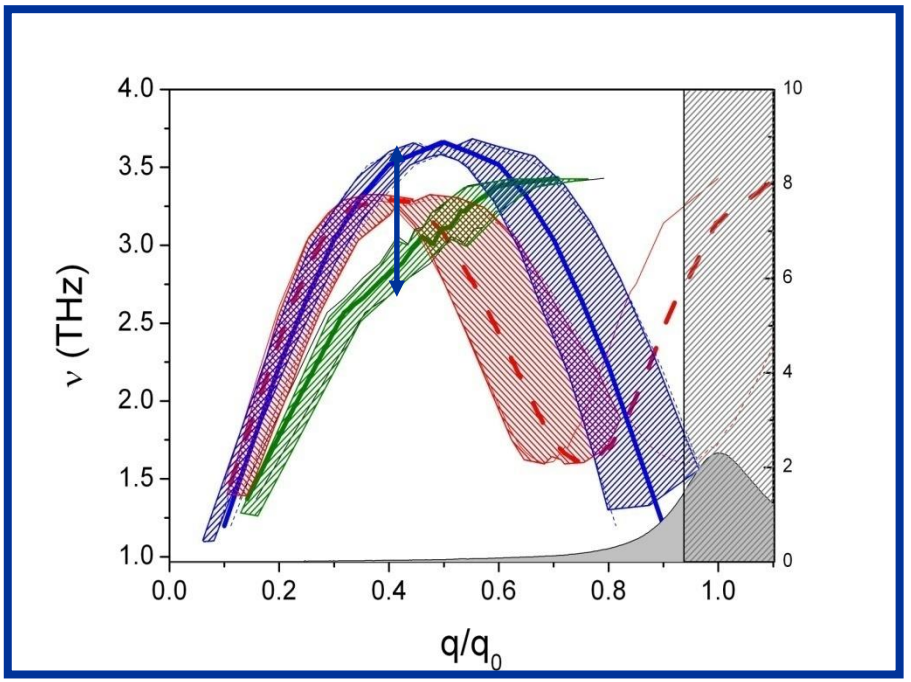

- **Local order → dispersion**
- **Average disorder → broadening**

Giordano & g.m., PNAS 107, 21985 (10)

The universal anomalies of glasses

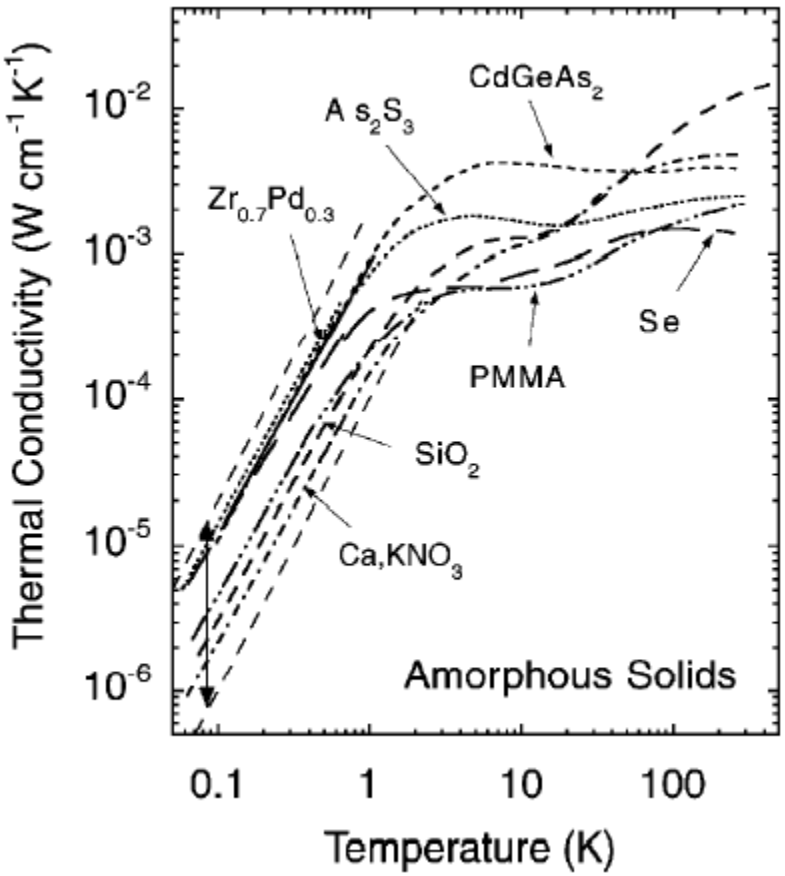

Pohl et al., Rev. Mod. Phys. 74, 991 (02)

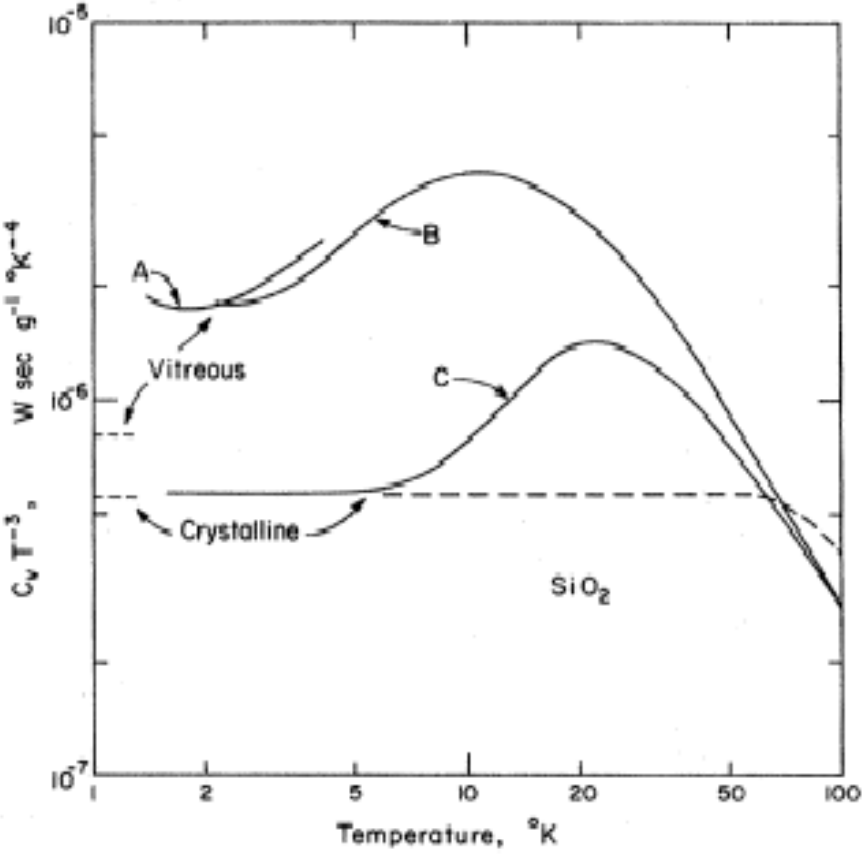

Zeller and Pohl, PRB 4, 2029 (71)

The dynamic structure factor of glycerol

Inelastic x-ray scattering data @ ID16, E=23.724 keV, ΔE=1.4 meV

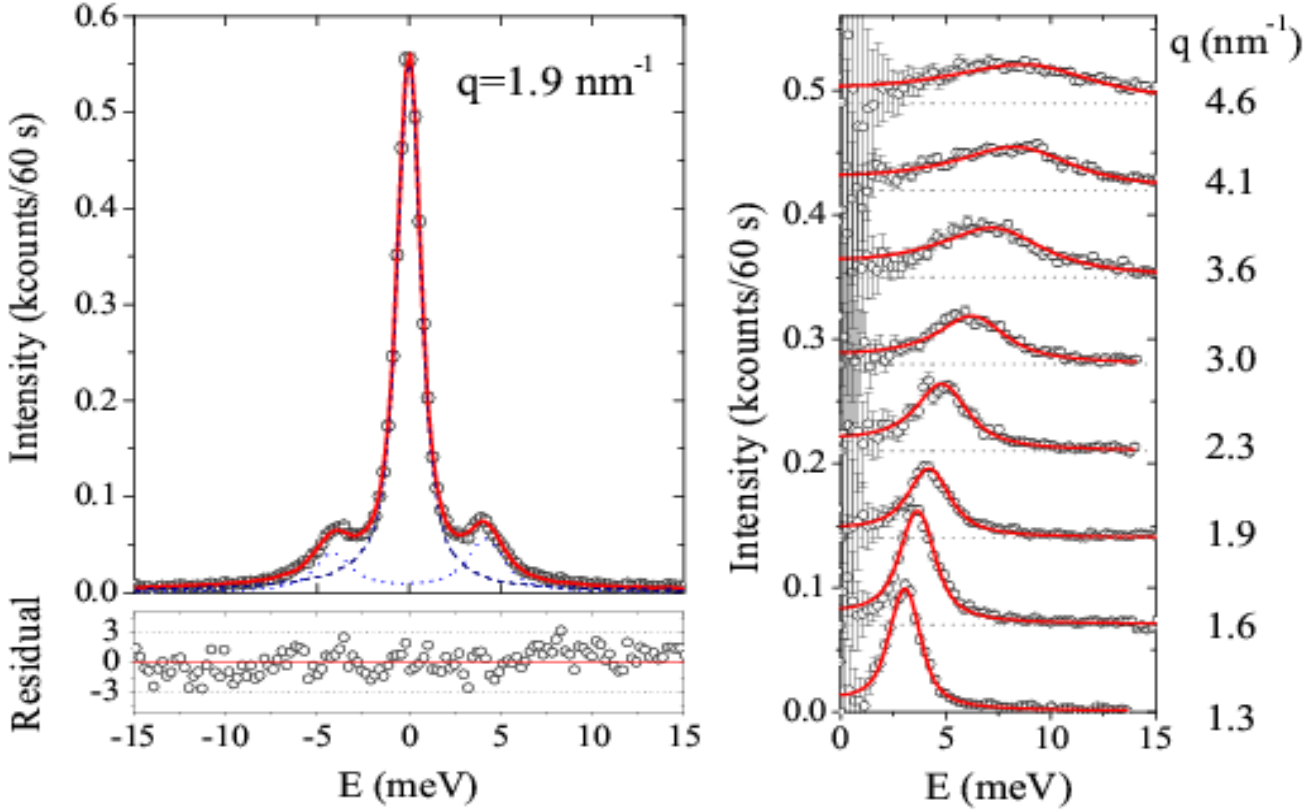

g.m. & Giordano, PNAS 106, 3659 (09)

Dispersion curve

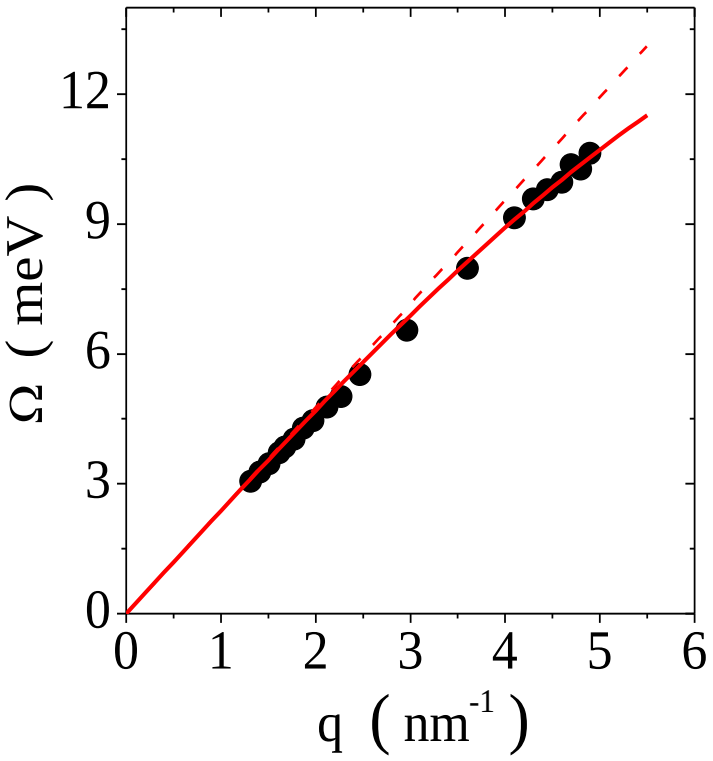

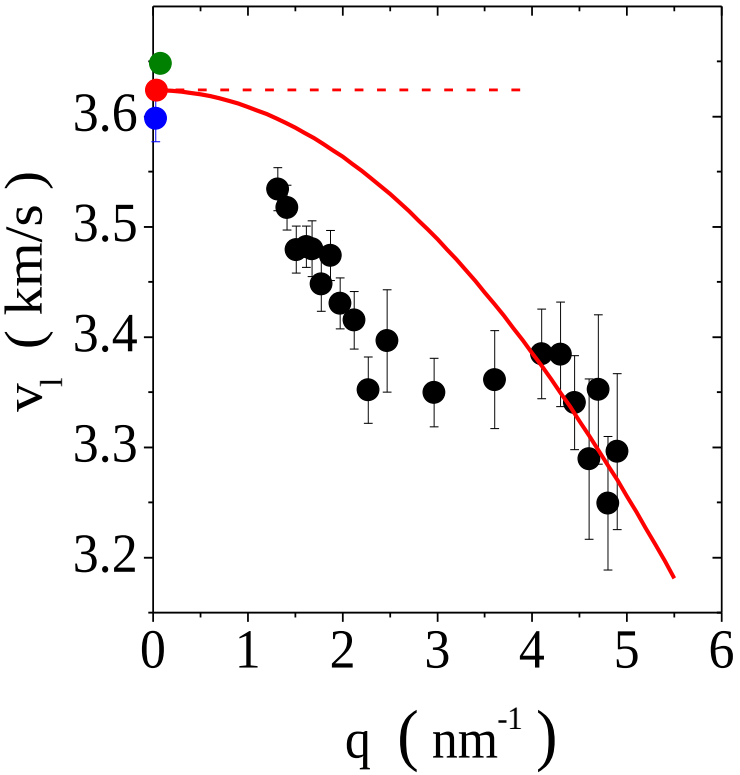

Low-frequency data from: Grubbs & MacPhail, JCP 100, 2561 (94);
Comez et al., JCP 119, 6032 (03); Masciovecchio et al., PRL 92, 247401 (04)

Acoustic attenuation

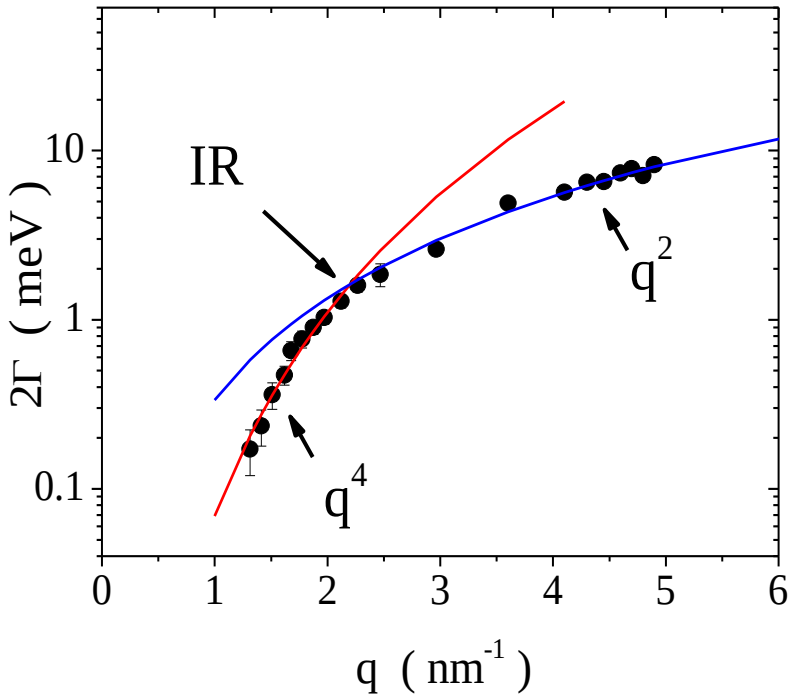

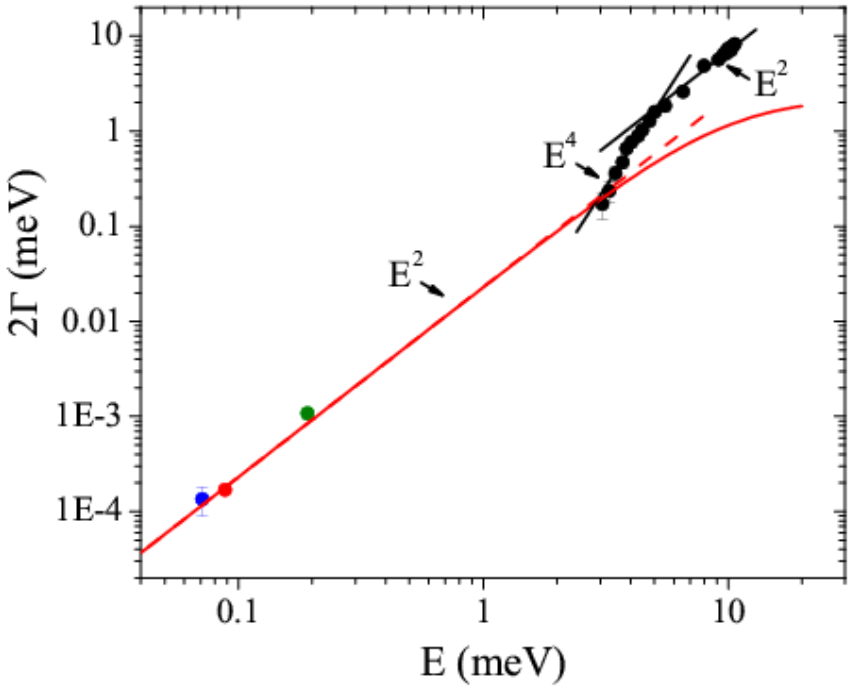

The q^4 to q^2 transition takes place close to the Ioffe-Regel limit defined as $\lambda_{IR}=2l$ ($\Omega/\pi=2\Gamma$)

anharmonic contribution:

$$2\,\Gamma = \frac{\gamma^2\, T\, C_v\, v_l\, \tau_{th}}{2\,\hbar\,\rho\, v_D^3}\; E^2$$

g.m. & Giordano, PNAS 106, 3659 (09)

The case of SiO_2: IXS

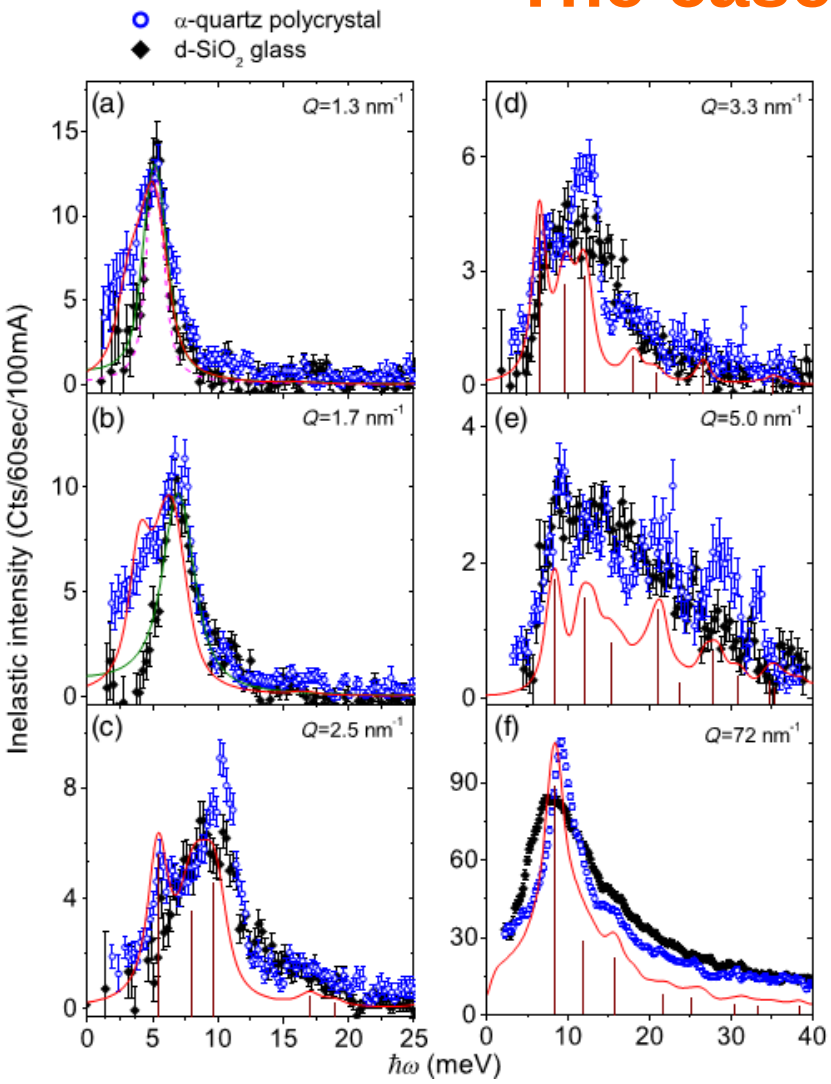

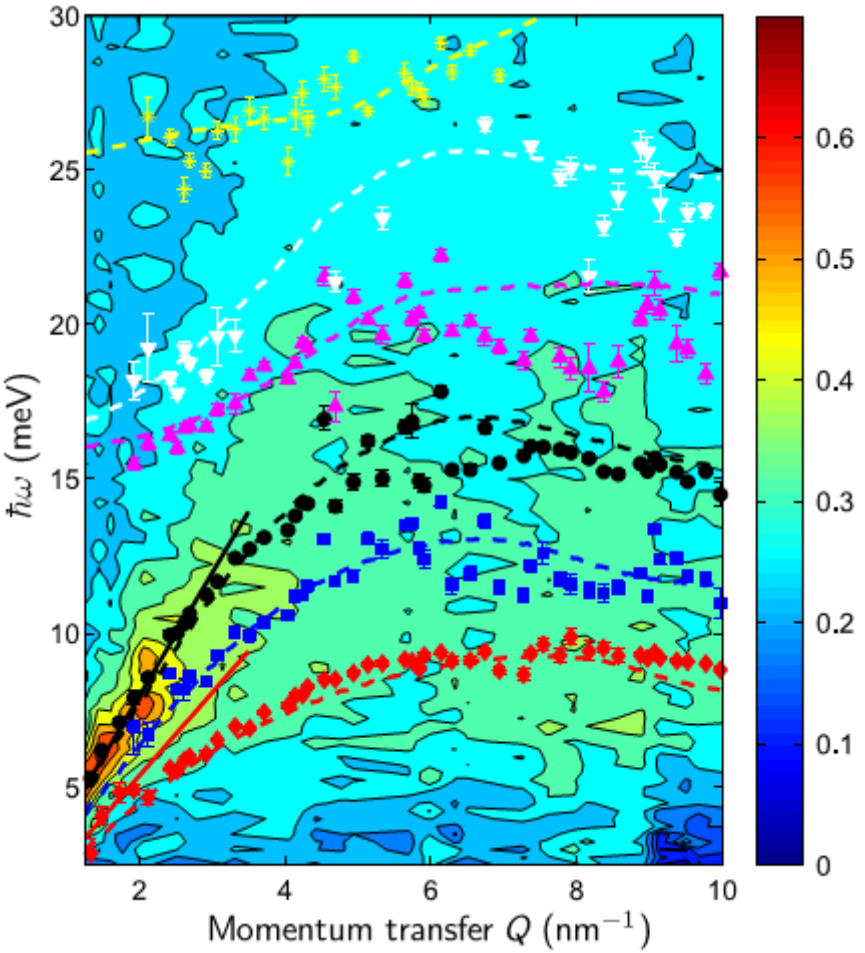

Baldi et al., PRL 110, 185503 (13)

Time domain interferometry

Relaxation process in liquids

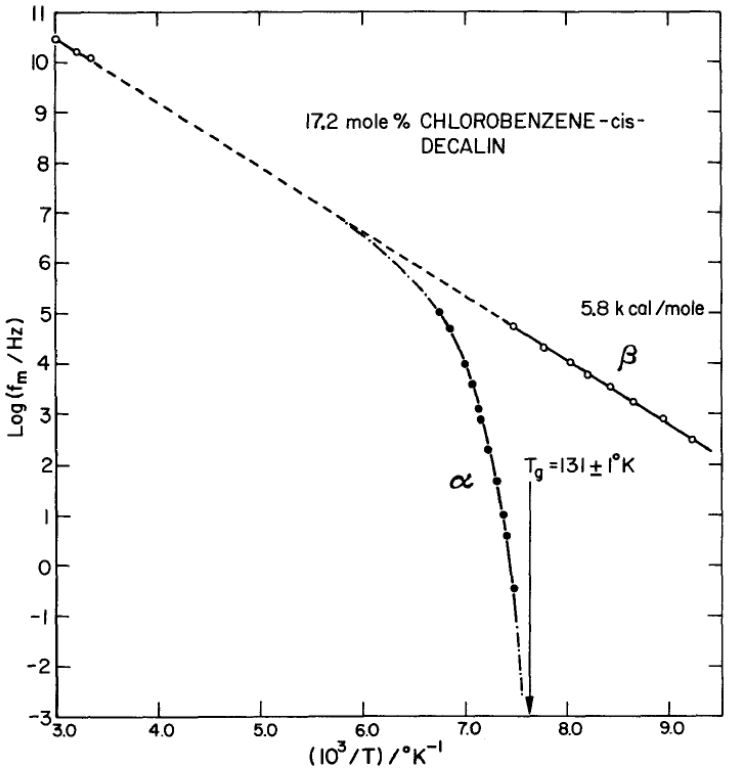

G. P. Johari , The Journal of Chemical Physics 58, 1766 (1973)

Main relaxations processes

α-relaxation

β-relaxation

Experimental challange:

to study slow dynamics (*n*s-μs) at the microscopic lenght scale

^{57}Fe

The nuclear fluorescence of ^{57}Fe has extraordinary properties:

$\Gamma = 4.66\ neV \rightarrow$ wide time window 1 ns – 10 μs

$E_\gamma = 14.414\ keV \rightarrow$ up to 14 A^{-1}

$\sigma = 246.40 \times 10^{-24}\ m^2$

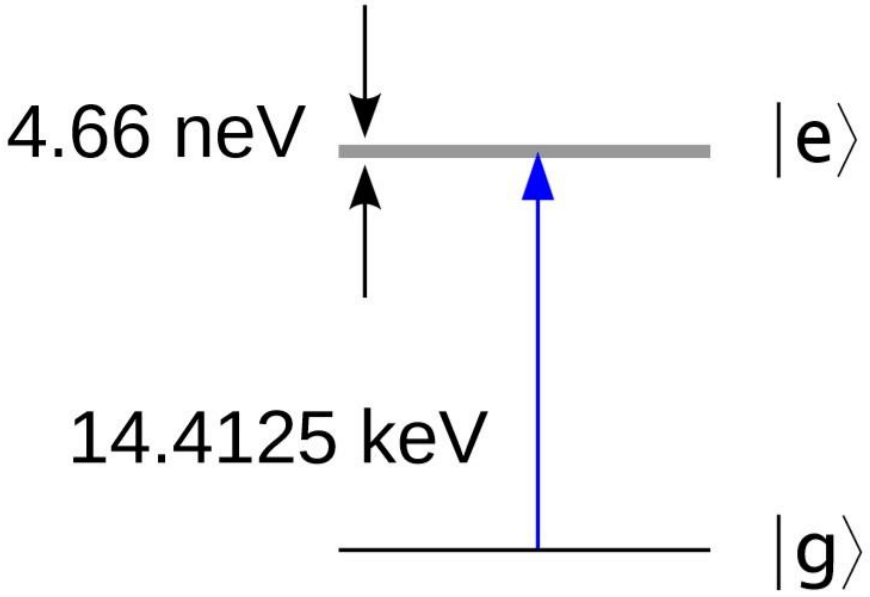

The technique

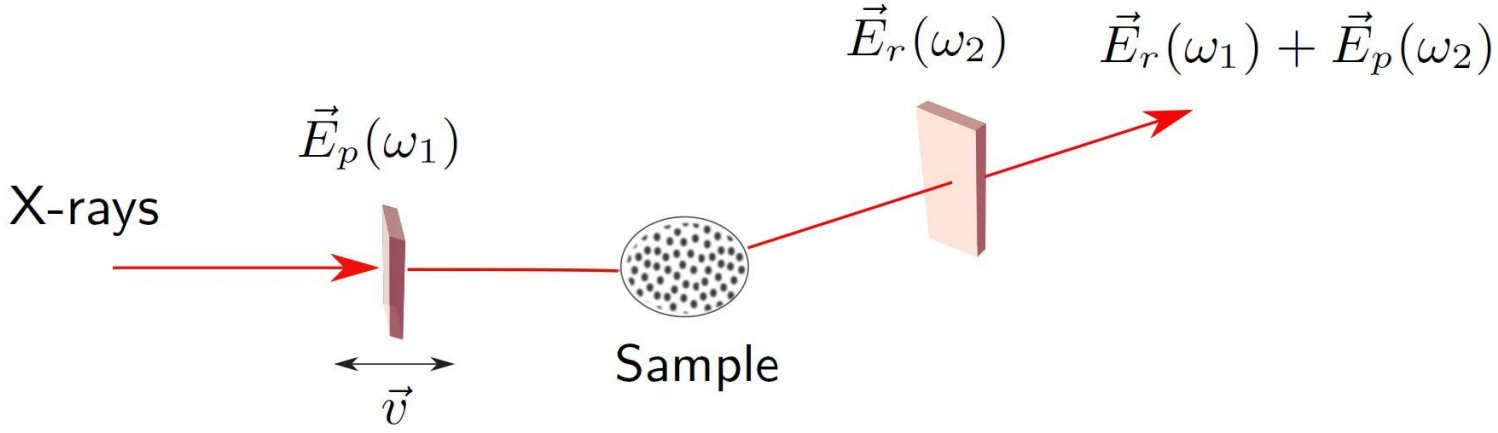

Arrival of SR pulse: $t = 0$

Detection of the nuclear fluorescence at t

The foils have two different excitation frequencies ω_1, ω_2

The sample response is given by $\rho_q(t)$

Scattering paths - I

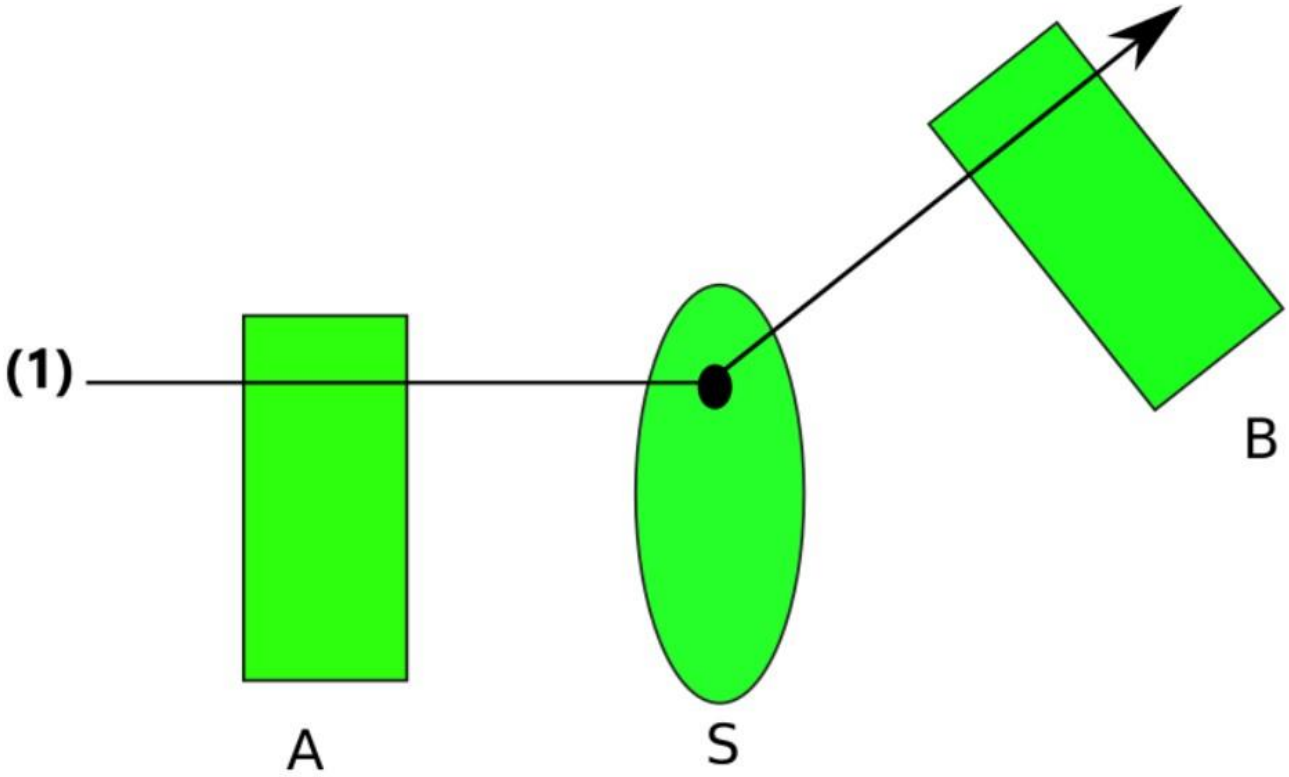

$$W_1 \propto \delta(t)\rho_q(t)$$

Scattering paths - II

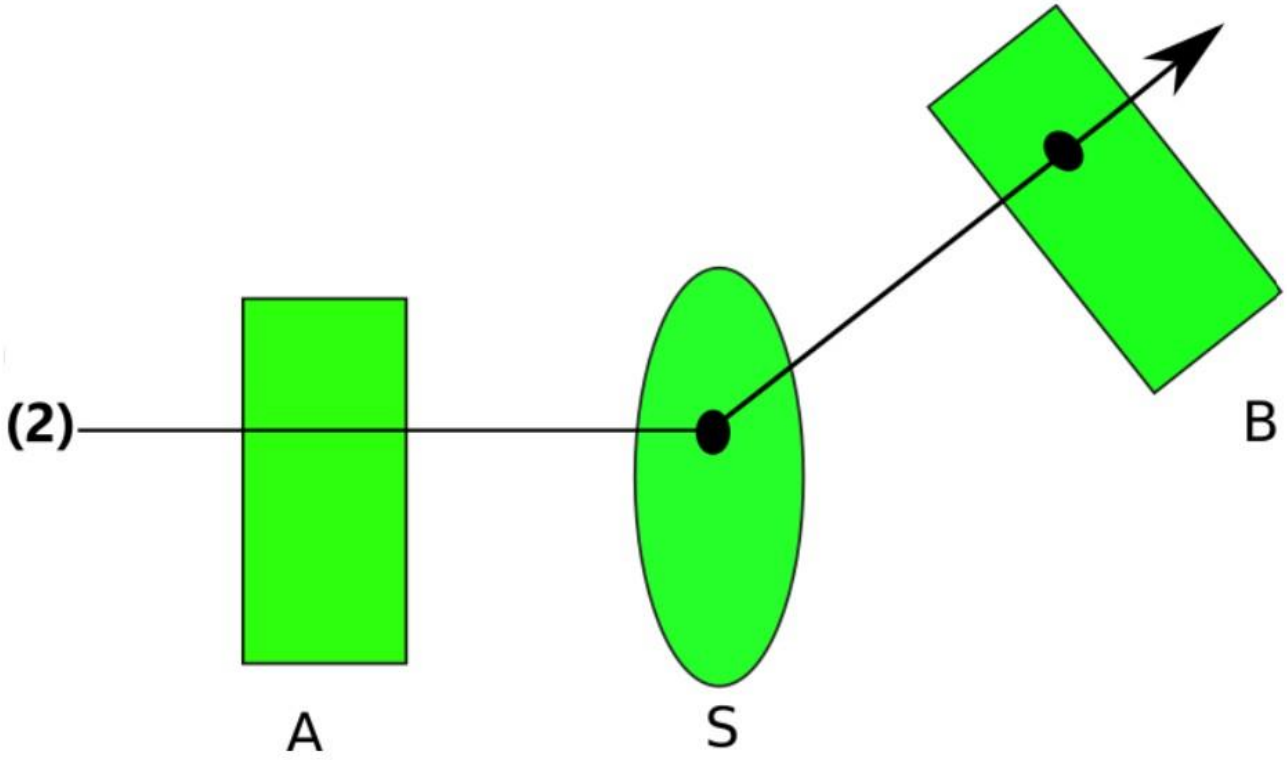

$$W_2 \propto e^{-i\omega_1 \left(t - \frac{t}{2\tau}\right)} \cdot \rho_q(0)$$

Scattering paths - III

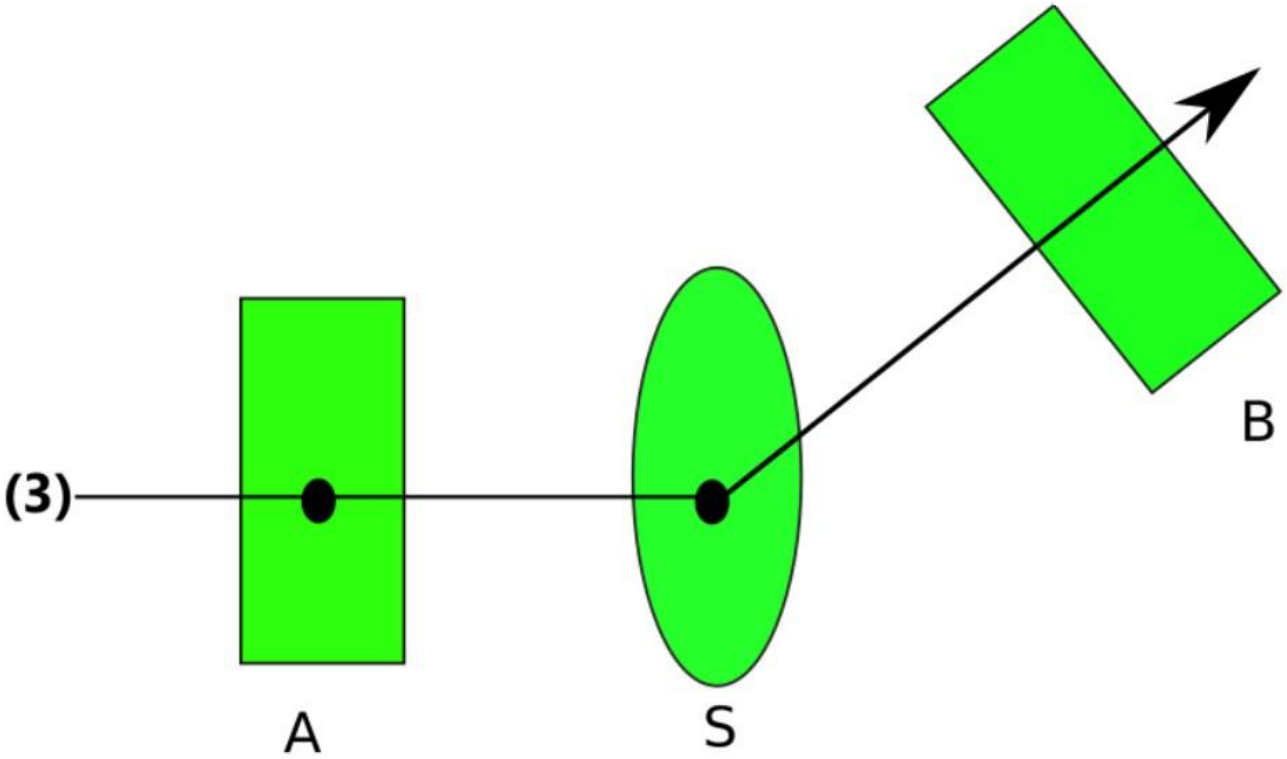

$$W_3 \propto e^{-i\omega_2 t - \frac{t}{2\tau}} \cdot \rho_q(t)$$

Scattering paths - summary

Intensity at the detector:

at each passage of the SR pulse a microstate m is probed

$$I_m(t) \propto |W_1 + W_2 + W_3|^2$$

I is then averaged over many SR pulses

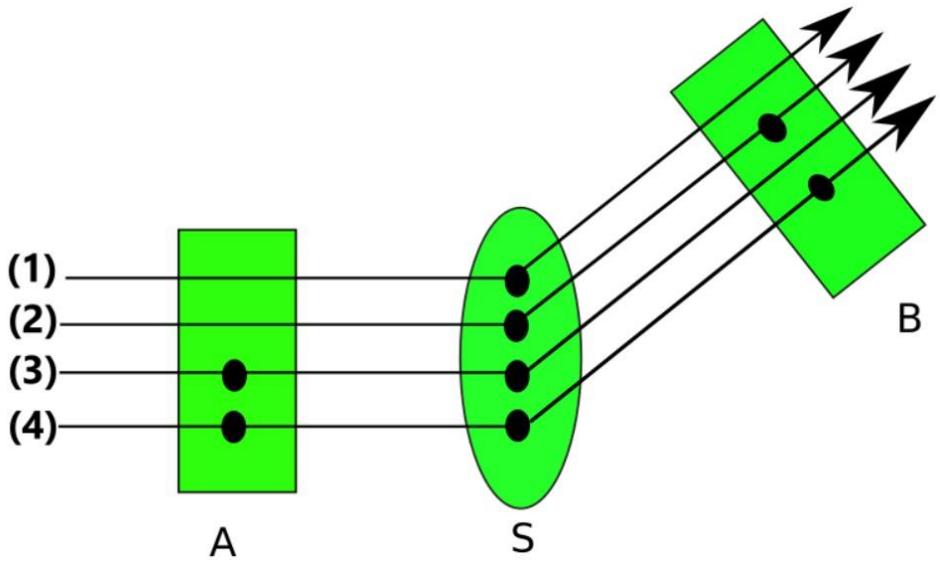

Scattering paths - summary

The final result gives:

$$(I_m)_m \propto e^{-\frac{t}{\tau}} \{1 + cos[(\omega_1 - \omega_2)t] \cdot (\rho_q(0)\rho_q(t))\}$$

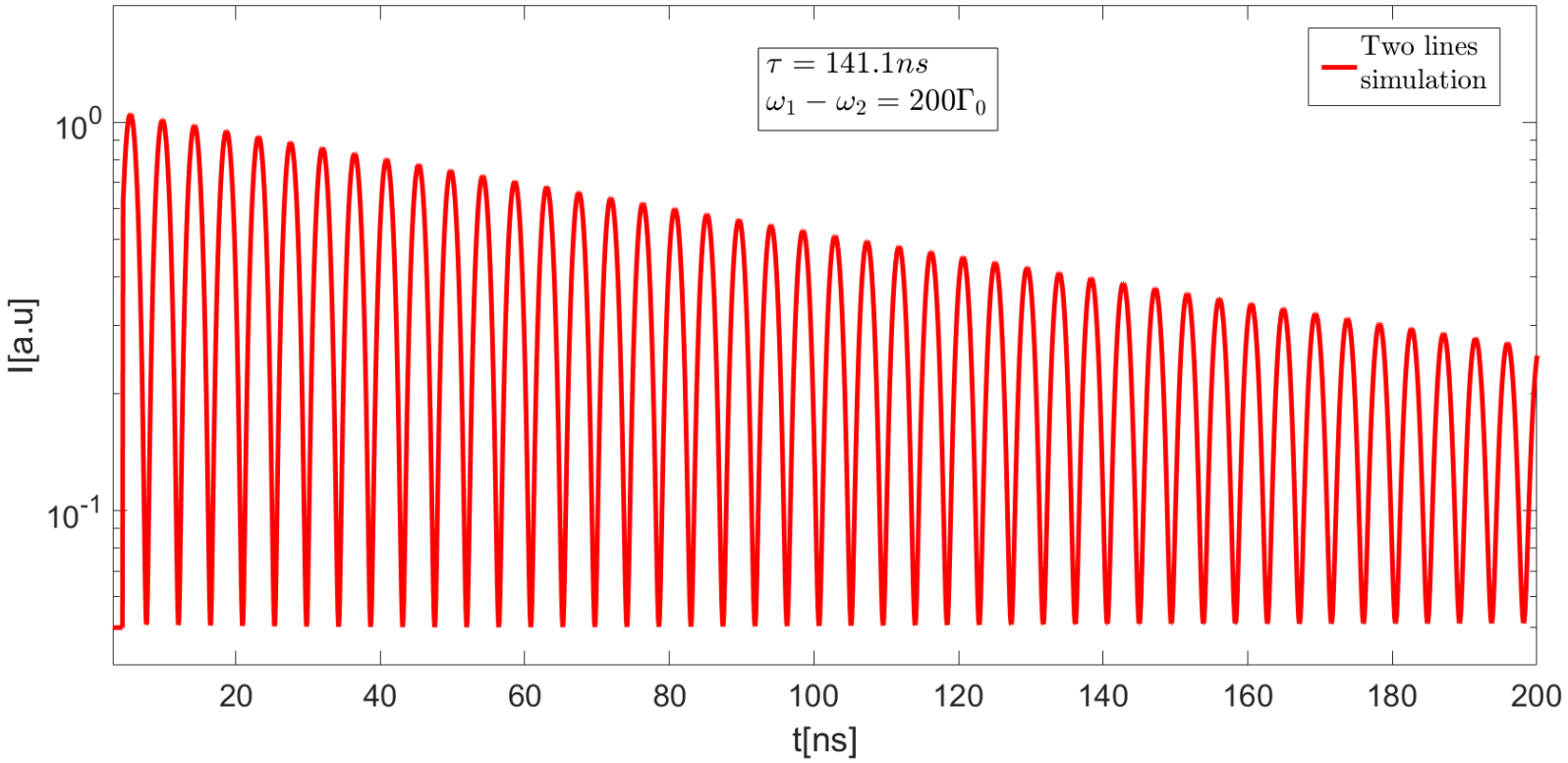

The case of 5-methyl-2-hexanol - I

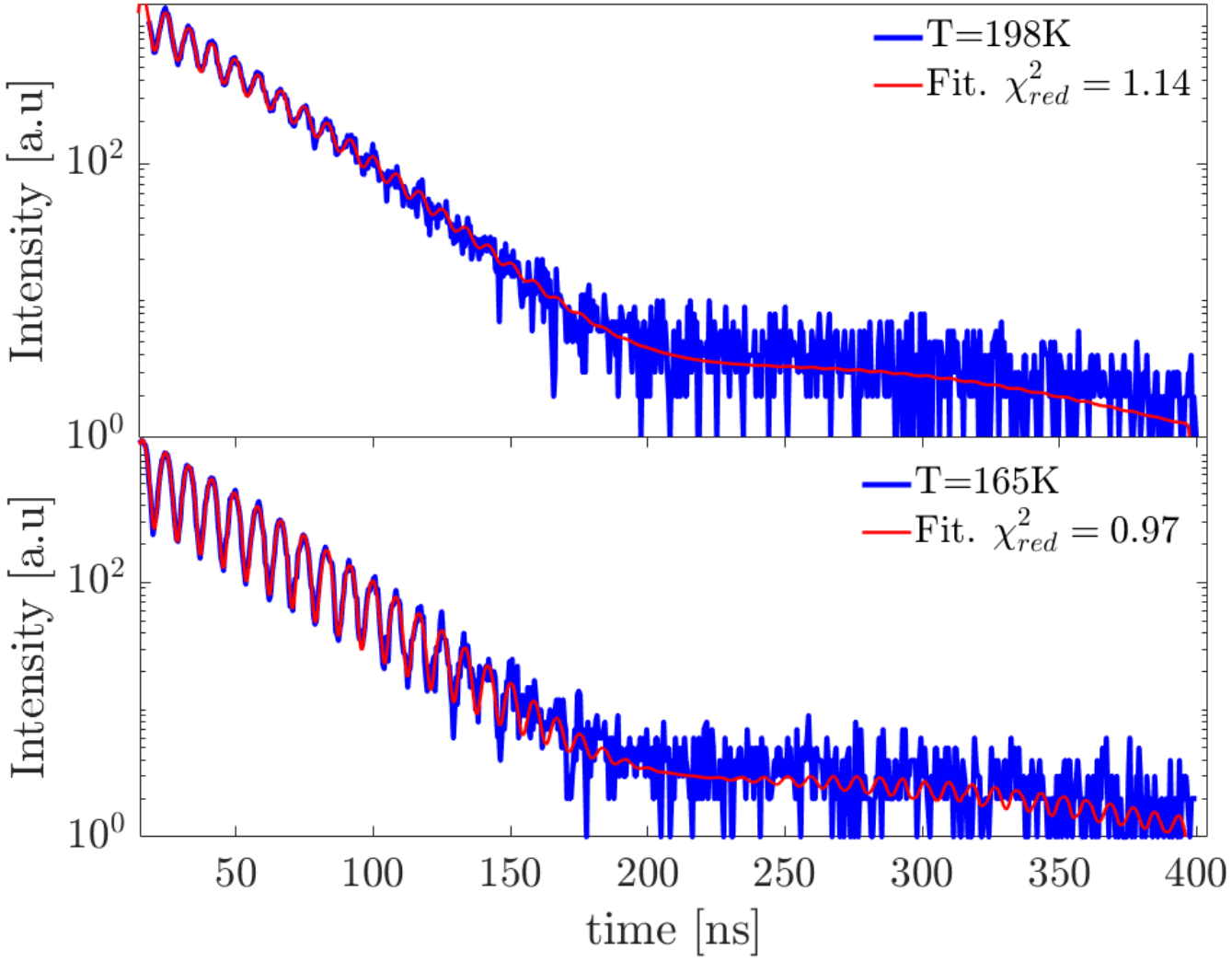

The case of 5-methyl-2-hexanol - II

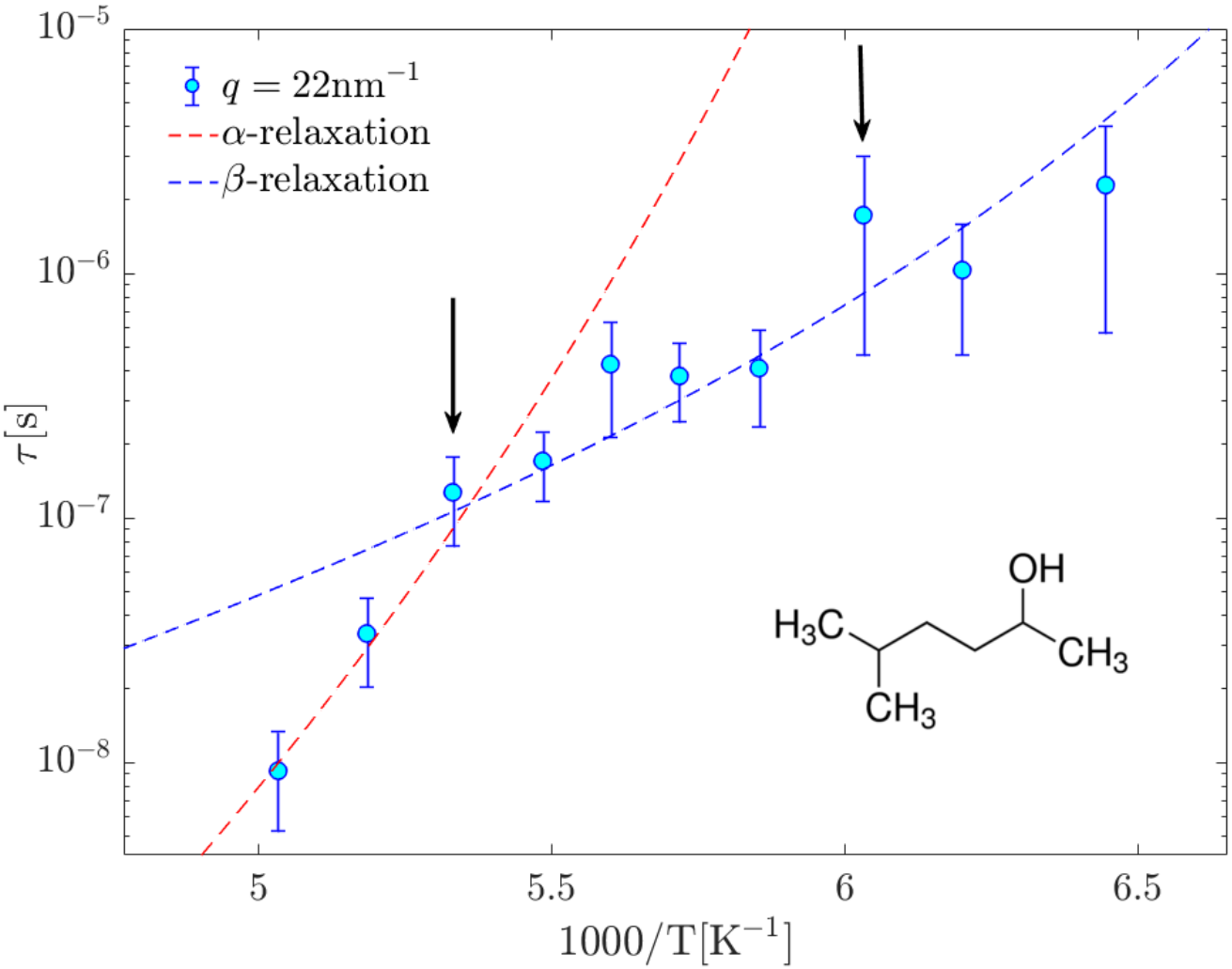

The case of 5-methyl-2-hexanol - III

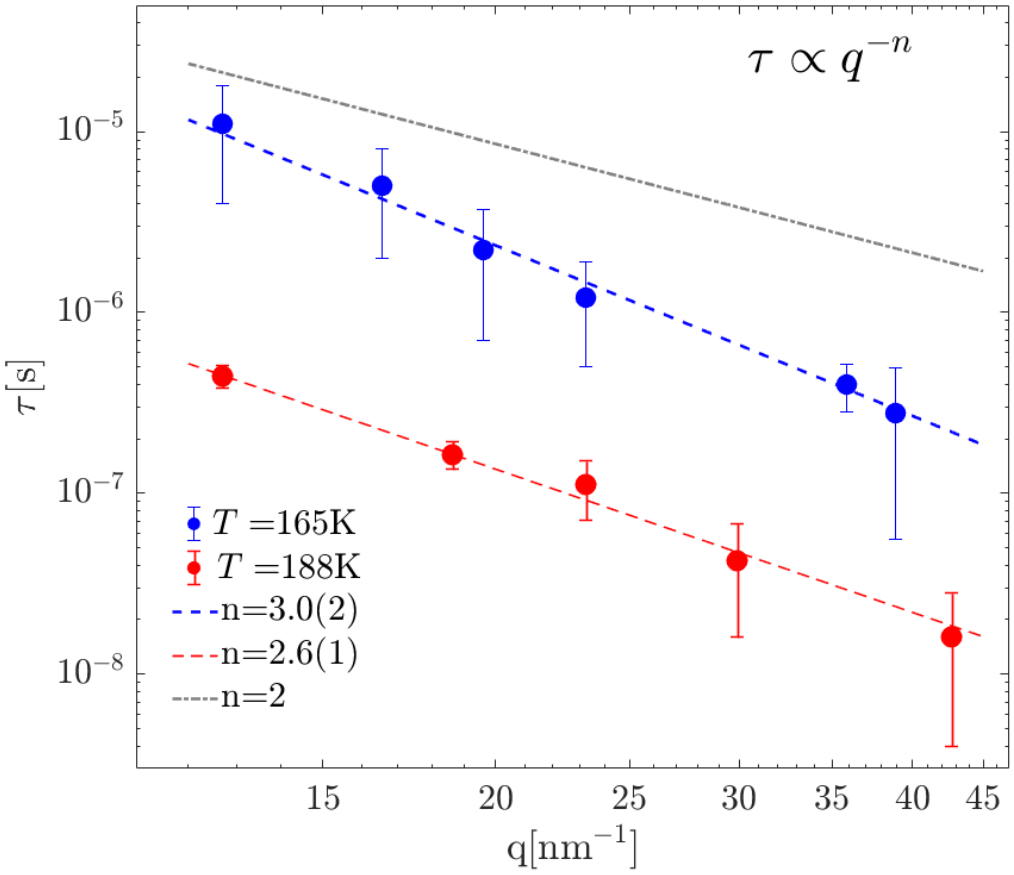

$n = 2 \Rightarrow$ Free diffusion

$n > 2 \Rightarrow$ Cooperative, restricted dynamics

Applications at FELs

First experiments ongoing @ LCLS

The LCLS creates X-ray pulses that can capture images of atoms and molecules in motion

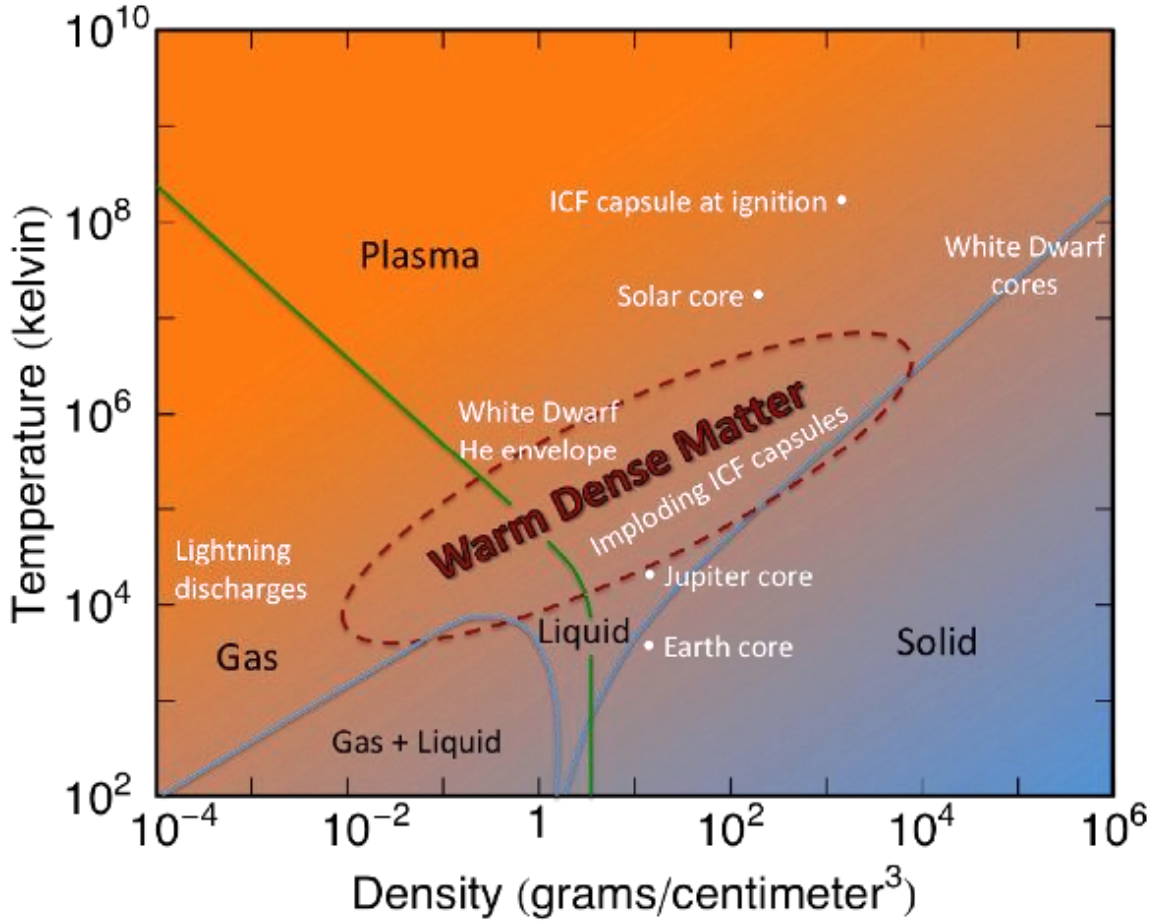

Uncertainties in transport coefficients of matter at extreme conditions are large – accurate estimates of viscosity would e.g. allow for more precise planetary models

5. First applications at FELs

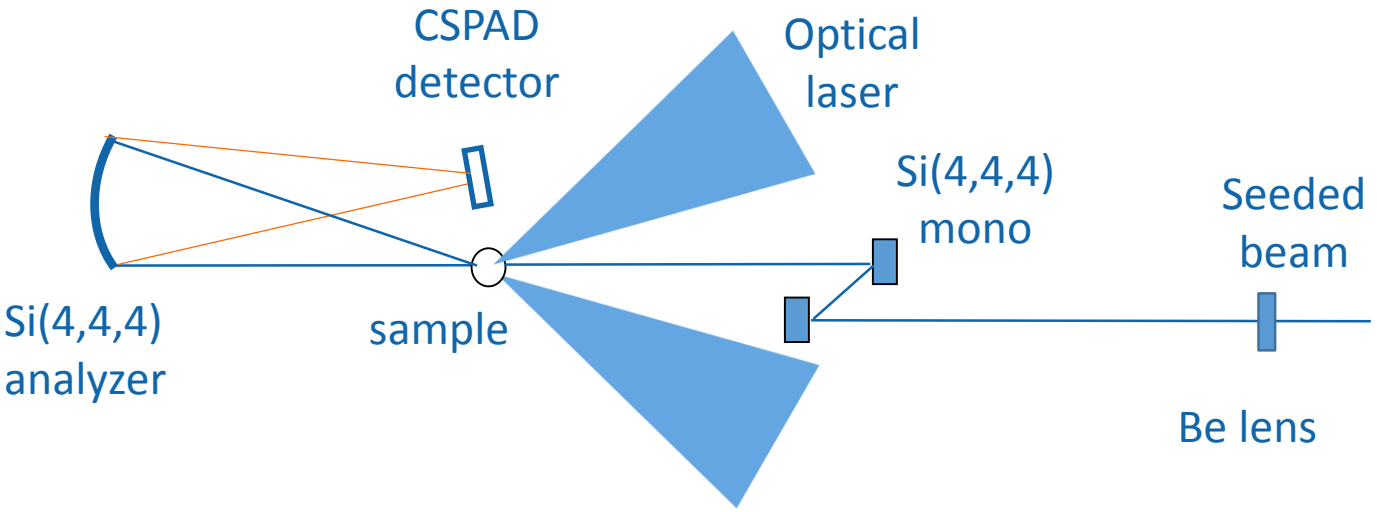

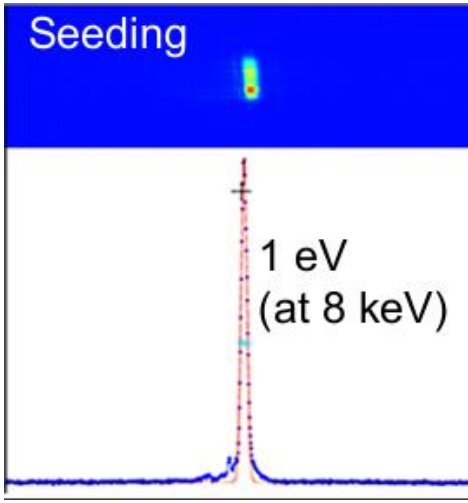

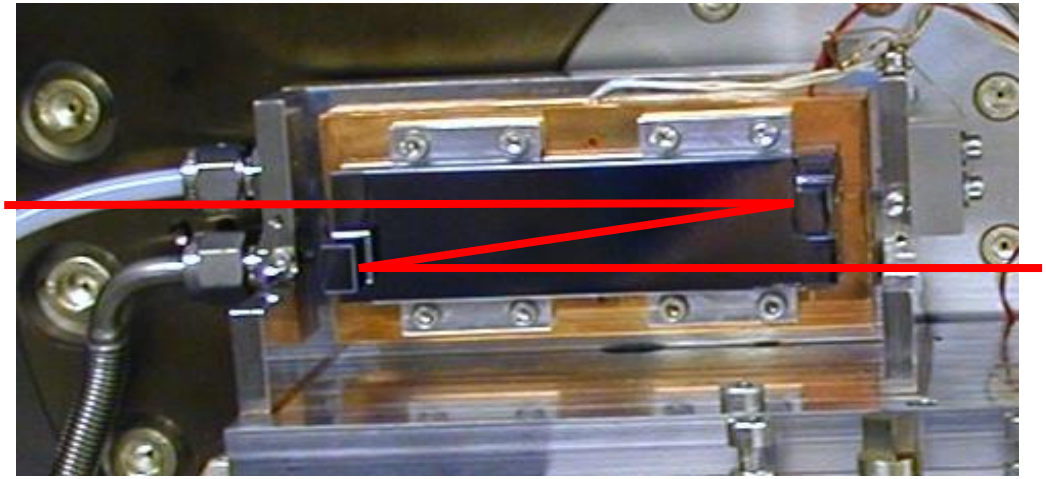

Si(4,4,4): $\Delta E/E=5\bullet10^{-6}$

Working conditions:
Bragg angle @ $\vartheta_{PM}=87^{o}$
$E_{PM}=7919.1$ eV
$\Delta E_{PM}\sim100$ meV

Sensitive to the seed crystal angle at the level of 0.001^{o}

5. First applications at FELs

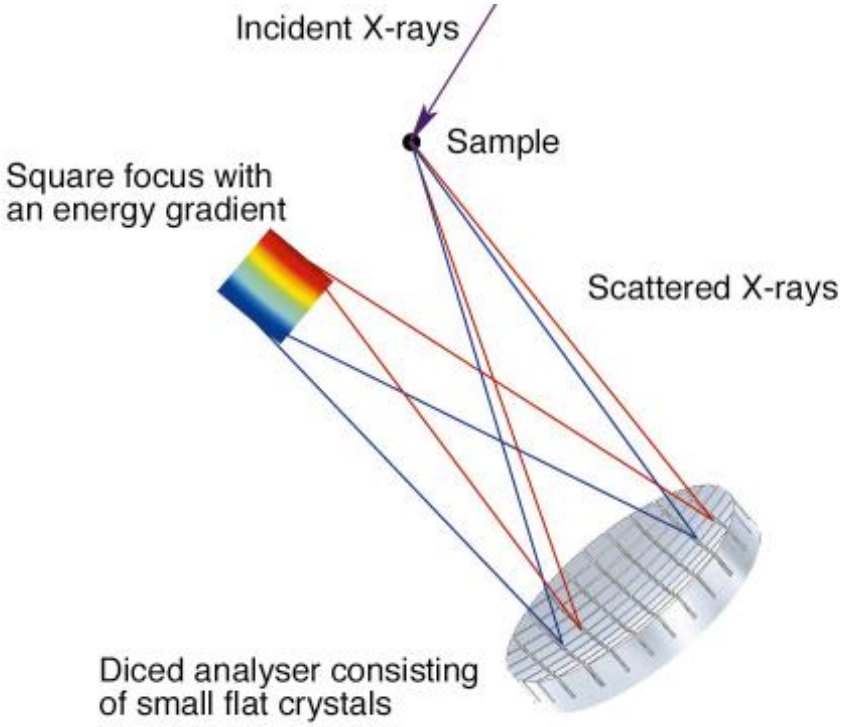

-~10.000 cubes of 0.7x0.7x2.3 mm^3
- perfect crystal properties
- collection of sufficient solid angle

@ MEC: CSPAD (110 μm pixel size) & diced Si(444) crystal with R=1 m & $\theta = 87^\circ \Rightarrow$ ~100 meV @ 7919 eV

Huotari et al., J. Synchrotron Rad. 12, 425 (2006)

Comparing experimental results and simulations:

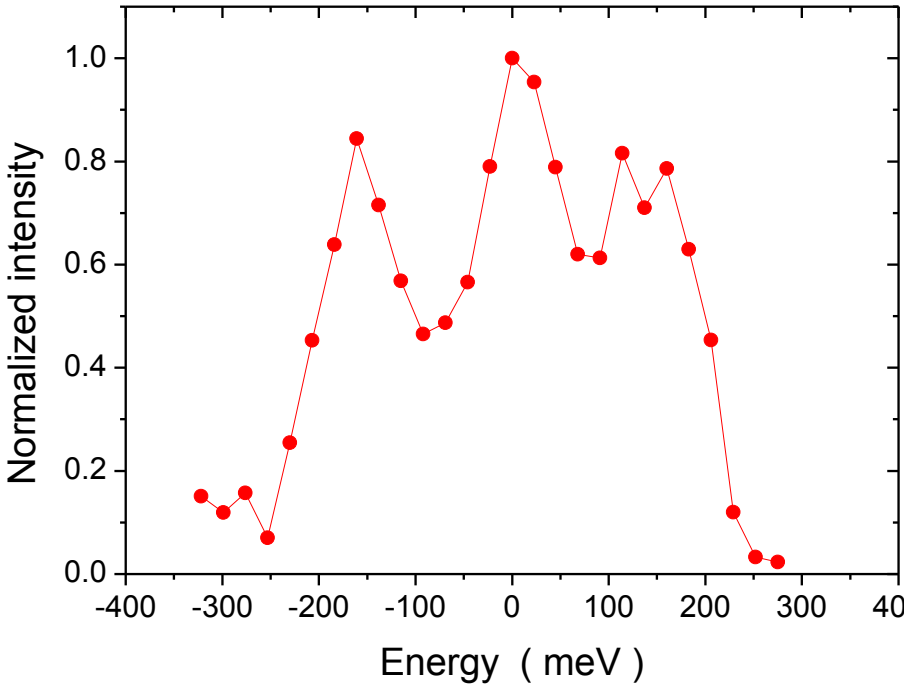

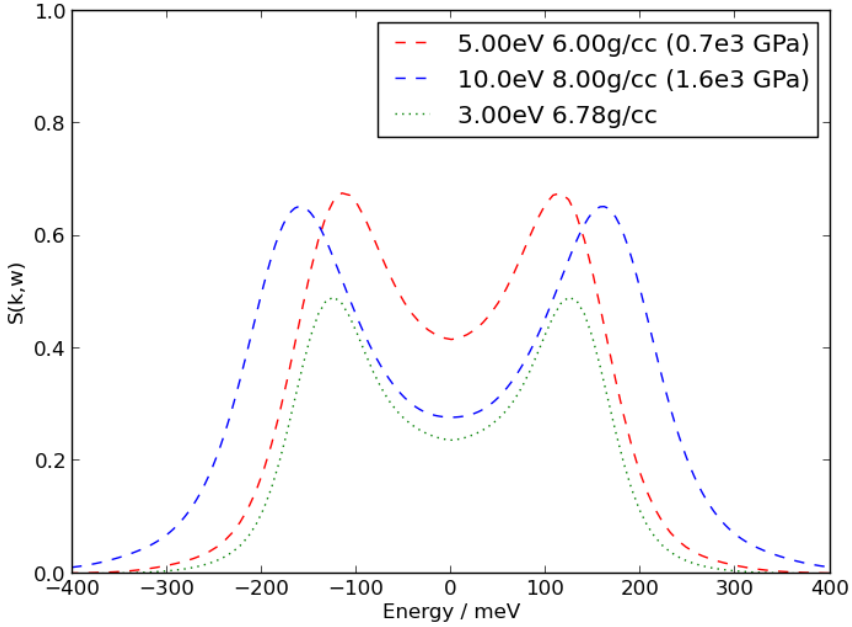

ab-initio quantum MD simulations (OF-DFT) describe pretty well the inelastic components. Where is the elastic one?